

Portability of genomic predictions trained on sparse factorial designs across two maize silage breeding cycles

Alizarine Lorenzi

INRAE UMR0320: Genetique Quantitative et Evolution Le Moulon

Cyril Bauland

INRAE UMR0320: Genetique Quantitative et Evolution Le Moulon

Sophie Pin

INRAE UMR0320: Genetique Quantitative et Evolution Le Moulon

Delphine Madur

INRAE UMR0320: Genetique Quantitative et Evolution Le Moulon

Valérie Combes

INRAE UMR0320: Genetique Quantitative et Evolution Le Moulon

Carine Palaffre

INRAE Nouvelle-Aquitaine Bordeaux: Institut National de Recherche pour l'Agriculture l'Alimentation et l'Environnement Centre Nouvelle-Aquitaine Bordeaux

Colin Guillaume

Maisadour

Gaëtan Touzy

RAGT2n

Tristan Mary-Huard

MIA-Paris: Mathematiques et Informatique Appliquees-Paris

Alain Charcosset

INRAE UMR0320: Genetique Quantitative et Evolution Le Moulon

Laurence Moreau

`laurence.moreau@inrae.fr`

INRAE: Institut National de Recherche pour l'Agriculture l'Alimentation et l'Environnement

<https://orcid.org/0000-0002-7195-1327>

Research Article

Keywords: Hybrid breeding, Genomic selection, Factorial design, Training set optimization, Inter-generation genomic prediction

Posted Date: September 6th, 2023

DOI: <https://doi.org/10.21203/rs.3.rs-3286945/v1>

License:  This work is licensed under a Creative Commons Attribution 4.0 International License.

[Read Full License](#)

Version of Record: A version of this preprint was published at Theoretical and Applied Genetics on March 7th, 2024. See the published version at <https://doi.org/10.1007/s00122-024-04566-4>.

Portability of genomic predictions trained on sparse factorial designs across two maize silage breeding cycles

Alizarine Lorenzi^{1,4}, Cyril Bauland¹, Sophie Pin¹, Delphine Madur¹, Valérie Combes¹, Carine Palaffre², Colin Guillaume³, Gaëtan Touzy⁴, Tristan Mary-Huard^{1,5}, Alain Charcosset¹, Laurence Moreau¹

¹ Université Paris-Saclay, INRAE, CNRS, AgroParisTech, Génétique Quantitative et Evolution - Le Moulon, 91190 Gif-sur-Yvette, France

² UE 0394 SMH, INRAE, 2297 Route de l'INRA, 40390, Saint-Martin-de-Hinx, France

³ Maïsadour Semences SA, F-40001 Mont-de-Marsan Cedex, France

⁴ RAGT2n, Genetics and Analytics Unit, 12510 Druelle, France

⁵ MIA, INRAE, AgroParisTech, Université Paris-Saclay, 75005, Paris, France

Corresponding author: Laurence Moreau laurence.moreau@inrae.fr. ORCID: 0000-0002-7195-1327

Abstract

Genomic selection offers new prospects for revisiting hybrid breeding schemes by replacing extensive phenotyping of individuals with genomic predictions. Finding the ideal design for training genomic prediction models is still an open question. Previous studies have shown promising predictive abilities using sparse factorial instead of tester-based training sets to predict single-cross hybrids from the same generation. This study aims to further investigate the use of factorials and their optimization to predict line general combining abilities (GCAs) and hybrid values across breeding cycles. It relies on two breeding cycles of a maize reciprocal genomic selection scheme involving multiparental connected reciprocal populations from flint and dent complementary heterotic groups selected for silage performances. Selection based on genomic predictions trained on a factorial design resulted in a significant genetic gain for dry matter yield in the new generation. Results confirmed the efficiency of sparse factorial training sets to predict candidate line GCAs and hybrid values across breeding cycles. Compared to a previous study based on the first generation, the advantage of factorial over tester training sets appeared lower across generations. Updating factorial training sets by adding single-cross hybrids between selected lines from the previous generation or a random subset of hybrids from the new generation both improved predictive abilities. The CDmean criterion helped determine the set of single-crosses to phenotype to update the training set efficiently. Our results validated the efficiency of sparse factorial designs for calibrating hybrid genomic prediction experimentally and showed the benefit of updating it along generations.

Keywords

Hybrid breeding, Genomic selection, Factorial design, Training set optimization, Inter-generation genomic prediction

33 **Key message (30 words)**

34 We validated the efficiency of genomic predictions calibrated on sparse factorial training sets to predict the next
35 generation of hybrids and tested different strategies for updating predictions along generations.

36 **Conflicts of interest**

37 The authors declare no conflict of interest.

38 **Acknowledgments**

39 We thank Lidea, Limagrain Europe, Maisadour Semences, Corteva, RAGT 2n, KWS and Syngenta Seeds grouped
40 in the frame of the ProMais SAM-MCR project for the funding, inbred lines development, hybrid production, and
41 phenotyping. We are also grateful to scientists from these companies and scientists of the INRAE-CIRAD “R2D2”
42 network for helpful discussions on the results. A.L. PhD contract was funded by RAGT 2n and ANRT contract n°
43 2020/0032, with the contribution of all SAM-MCR project partners. GQE-Le Moulon benefits from the support
44 of Saclay Plant Sciences-SPS (ANR-17-EUR-0007).

45

46 **Introduction**

47 Maize varieties are generally single-cross hybrids obtained by crossing two inbred lines that belong to
48 complementary heterotic groups. The challenges for breeders are (i) selecting lines within each heterotic group
49 that will be used as parents for the next generation and (ii) identifying the best single-cross hybrids among all
50 possible ones in order to derive new varieties. The advent of Doubled-Haploid (DH) technology now enables the
51 rapid production of numerous fully homozygous inbred lines each year. This large number of candidate lines
52 produced each year in breeding programs makes generating and evaluating all potential single-cross hybrids
53 practically undoable. To overcome this difficulty, conventional maize hybrid breeding schemes are typically
54 divided into two stages. In the first stage (1), topcross hybrids are produced by crossing candidate lines from one
55 heterotic group with a limited number of inbred lines from the complementary group, referred to as "testers". The
56 performances of these topcross hybrids provide an estimation of the general combining abilities (GCA) of the
57 candidate lines. In the second stage (2), the selected lines from stage 1 are crossed using a sparse factorial design
58 to identify the best single-cross hybrid combinations. At this stage, the selection is performed on the GCA of the
59 parental lines and the specific combining ability (SCA) of the pair of parental lines. Selecting lines based on a
60 limited number of testers at stage 1 does not fully exploit the complementarity between the candidate lines from
61 the two heterotic groups and can bias the line GCA estimation since the line GCA and its SCAs with the testers
62 are confounded (Hallauer et al. 2010). Also, the two-stage process is time-consuming and requires extensive
63 phenotyping (at least as many as the total number of candidate lines in both groups in stage 1).

64 Due to limited resources for phenotyping, predicting the performance of untested hybrids has been a
65 critical objective in hybrid selection. Bernardo (1994) was the first to propose a marker-based model for plant
66 hybrid performance prediction. He combined marker-based distances between parental lines of hybrids and the
67 performances of a related set of single-crosses to predict GCAs and SCAs of non-phenotyped hybrids. This
68 prediction model, which aims at predicting the value of unphenotyped individuals based on their marker-based
69 relationship with a set of individuals both phenotyped and genotyped, is similar to the genomic best linear unbiased
70 prediction (GBLUP) model (VanRaden 2008) that has been proposed more recently and is now widely used to
71 perform genomic selection (GS) in plants and animal. Different other genomic prediction models have been
72 proposed (see Meuwissen et al. 2001 seminal paper and Howard et al. 2022 for a review), all of them use molecular
73 markers scored across the entire genome to predict the genetic values of genotyped individuals, referred to as the
74 prediction set (PS), using individuals both phenotyped and genotyped, referred to as the training set (TRS). Since
75 the pioneer work of Bernardo (1994), different prediction models adapted to hybrid value prediction have been

76 proposed considering non-additive effects, either by modeling the GCA and SCA effects or the additive,
77 dominance, and epistasis effects (Vitezica et al. 2013, 2017; Varona et al. 2018; González-Diéguéz et al. 2021).
78 Even if several studies have confirmed the efficiency of these GS models for predicting single-cross hybrid values
79 in maize (see review by Kadam and Lorenz 2018), the relative interest of the different prediction models is still
80 unclear. Besides the statistical model, various factors are known to affect genomic prediction accuracies, such as
81 trait heritability, the number of markers, the size of the TRS, and the relationship between the TRS and the PS (see
82 reviews: Kadam and Lorenz 2018; Isidro y Sánchez and Akdemir 2021; Merrick and Carter 2021; Kadam et al.
83 2021). In the context of hybrid prediction, in addition to these factors, the crossing design used to produce the TRS
84 hybrids also affects prediction accuracy (Technow et al. 2014; Seye et al. 2020; Lorenzi et al. 2022).

85 In most studies, GS for hybrid value prediction has been considered in the second stage of the hybrid
86 breeding scheme, i.e., by using as TRS hybrids between lines that have already undergone a selection based on
87 their testcross values. To improve the efficiency of hybrid breeding schemes, Kadam et al. (2016) and (Giraud
88 2016) proposed (1) to replace topcross evaluation in stage 1 with a sparse factorial design between unselected
89 candidate lines from both groups and (2) to use GS to predict GCAs of all lines and SCA of all potential single-
90 cross combinations. This makes it possible to perform selection in one stage instead of two. Both studies found
91 good prediction accuracies for untested hybrids using factorial designs as TRS. Later, simulations and
92 experimental studies have shown the potential of using sparse factorial instead of tester TRSs when predicting the
93 same generation (Seye et al. 2020; Burdo et al. 2021; Lorenzi et al. 2022). Although a simulation work validated
94 the advantage of factorial compared to tester TRSs to predict hybrid values across breeding cycles (Seye et al.
95 2020), further experimental validation is needed. From one cycle to the next, the average relatedness between the
96 TRS and PS decreases and the joint effect of selection, drift, and recombination events change allele frequencies
97 and the linkage disequilibrium between markers and QTLs, which decrease prediction accuracy if the TRS is not
98 updated along cycles (Pszczola et al. 2012; Isidro y Sánchez and Akdemir 2021; Rio et al. 2022b). This raises
99 questions about how to efficiently update the TRS to maximize prediction accuracy while minimizing phenotyping
100 costs.

101 According to the literature, an ideal TRS should maximize the accuracy by maximizing the relationship
102 between the TRS and PS (Zhong et al. 2009; Zhao et al. 2012; Technow et al. 2013) and minimizing the within
103 TRS relationship to capture a large genetic variance (Pszczola et al. 2012; Isidro y Sánchez and Akdemir 2021).
104 Different optimization criteria have been proposed to define the TRS (Rio et al. 2022b). Rincent et al. (2012)
105 proposed optimizing the TRS by maximizing the mean of the coefficient of determination (CDmean) of contrasts

106 between each unphenotyped PS individual and the target population mean. Numerous studies have shown that
107 building the TRS using the CDmean significantly increases the accuracy of GS models relative to random sampling
108 (Isidro y Sánchez and Akdemir 2021; Rio et al., 2022; Fernández-González et al. 2023). In a breeding program,
109 where genomic prediction is applied routinely, a large dataset from previous years of phenotyping is available for
110 model training. One can wonder which phenotypic data from the previous generation(s) should be included in the
111 TRS and which additional hybrids should be phenotyped to complete the existing TRS and achieve the highest
112 prediction accuracy for the new generation with a given phenotyping effort. One idea could be to use the CDmean
113 to optimize the choice of the individuals from the new generation to be phenotyped while considering the existing
114 TRS comprising data from the previous generations. To our knowledge, this strategy has never been tested in this
115 context.

116 The present study investigates the use and optimization of factorial TRS for genomic prediction of hybrid
117 performance across breeding cycles. It relies on two breeding cycles of a reciprocal genomic selection scheme
118 initiated from multiparental connected reciprocal populations generated in the flint and dent complementary
119 heterotic groups. Data from the first cycle was already analyzed in previous studies (Giraud et al. 2017a, b; Seye
120 et al. 2019) and have shown promising results in terms of genomic predictive abilities for replacing testcross
121 evaluation by sparse factorial evaluations (Lorenzi et al. 2022). We present in study results from a new breeding
122 cycle that was produced and evaluated in a factorial design to: (i) estimate the genetic gain achieved after selection
123 based on genomic predictions calibrated on a sparse factorial, (ii) assess the predictive ability in the new breeding
124 cycle and compare different GS models, (iii) evaluate the efficiency of training GS models on a factorial design
125 for predictions across breeding cycles and compare it to tester designs, (iv) investigate the benefit of different
126 strategies to update the factorial TRS across cycles and optimize it to predict the new generation.

127 **Materials and Methods**

128 This study relies on data from a reciprocal breeding experiment aiming at improving the silage performance of
129 maize single-cross hybrids produced between the dent and flint heterotic groups, the two main heterotic groups
130 used for silage maize hybrids in Northern Europe. The experimental data comprises two breeding cycles, further
131 called G0 and G1. Inbred lines from the G0 cycle were evaluated for hybrid performances in three experimental
132 designs already analyzed in previous publications (Giraud et al. 2017a, b; Seye et al. 2019; Lorenzi et al. 2022). A
133 summary of the G0 cycle production is provided below. The best G0 lines in each group were selected based on

134 genomic predictions and intercrossed to produce the new breeding cycle (G1) we will focus on in this study. All
135 experimental designs are described in **Table 1** and **Fig.1**.

136 **Summary of the G0 plant material production and selection of the best candidate lines**

137 Four founder lines were intercrossed in each group to derive six biparental families. In total, 822 flint lines and
138 802 dent lines were produced, further called G0 lines. The G0 lines were crossed to produce three experimental
139 hybrid designs. The G0_F-1H was obtained by crossing the 822 flint lines to the 801 dent lines following a sparse
140 factorial design, leading to 951 single-cross hybrids (on average, one line contributed to 1.2 hybrids). This
141 experimental design was evaluated in France and Germany in 2013 and 2014 for silage performances (Giraud et
142 al. 2017a, b; Seye et al. 2019). Then, 30 G0 lines were selected in each heterotic group based on genomic
143 predictions trained on the G0_F-1H for an index combining silage yield, moisture content at harvest, and silage
144 quality. Additionally, 60 G0 lines (10 lines per family) were chosen randomly. These lines were used to create two
145 other experimental designs. The G0_F-4H factorial design composed of 363 hybrids (on average, one line
146 contributed to four hybrids) was produced by randomly crossing (i) the 30 G0 selected flint lines to the 30 G0
147 selected dent lines to produce 131 hybrids (further called “G0S hybrids”) and (ii) the 60 G0 random dent lines to
148 the 60 G0 random flint lines leading to 232 hybrids (further called “G0R hybrids”). In parallel, the G0_T-F (and
149 G0_T-D) tester design was produced by crossing the same 90 G0 flint (dent) lines from one group to two founder
150 lines from the dent (flint) group used as testers. Together, the G0_T-F and G0_T-D tester designs were called G0
151 tester designs or G0_T. The G0_F-4H and the G0_T were evaluated jointly in eight trials in Northern France and
152 Germany in 2016 and 1017 (Seye 2019; Lorenzi et al. 2022). In all trials, 18 hybrids were used as controls and
153 evaluated twice: two commercial hybrids (LG30.275 and RONALDINIO) and 16 founder hybrids produced by
154 crossing the four flint founder lines with the four dent founder lines.

155 **New breeding cycle (G1)**

156 40 intragroup single-crosses were produced in each group by crossing the 30 selected G0 lines described above.
157 351 dent and 351 flint DH lines (G1) were derived from the 40 single-crosses in the dent and flint groups,
158 respectively. The dent G1 lines were crossed with the flint G1 lines following a sparse factorial design to produce
159 442 G1 hybrids. Crosses were made at random with an average number of hybrids per line close to one. A new set
160 of 47 G0S hybrids between the 30 G0 selected lines from each group was produced and evaluated jointly with the
161 G1 hybrids, yielding a total of 489 hybrids further referred to as (G0S+G1)_F-1H. Hybrids were evaluated for two
162 years in the North of France and Germany: three trials in 2019 and five in 2020. The same 18 control hybrids (two

163 commercial and 16 founder hybrids) as in the G0 experiments were evaluated twice in each trial. 15% of the
164 experimental hybrids were also replicated once at each location. The field experiments were laid out as augmented
165 partially replicated designs (p-rep) (Williams et al. 2011). Each trial comprised 512 to 520 elementary plots
166 distributed in 26 incomplete blocks of 20 plots. Each genotype was evaluated in 7 trials across 2019 and 2020 and
167 was replicated in at least one trial. For each trial, repetitions were allocated to blocks to form an efficient
168 incomplete block design using the DiGger R package (Coombes 2009).

169 Hybrids were evaluated for 11 traits, four agronomical traits: silage yield (DMY in tons of dry matter per
170 ha), dry matter content at harvest (DMC in % of fresh weight), female flowering date (DtSilk in days after January
171 the first) and plant height (PH in cm) and seven silage traits for digestibility: milk fodder unit per kilogram of dry
172 matter (MFU in MFU per kg) (Andrieu 1995) (computed using model 4.2), cell wall content of the harvested dry
173 matter measured by the neutral detergent fiber content (NDF in % of dry matter), cell wall in vitro digestibility of
174 the non-starch and non-soluble carbohydrates part of silage (DINAG in %) and cell wall in vitro digestibility of
175 the non-starch, non-soluble carbohydrates and non-crude protein part of silage (DINAGZ in %), lignin, cellulose
176 and hemicellulose contents in the cell wall NDF evaluated with the Goering and Soest (1970) method (LIGN,
177 CELL, and HCELL in % of NDF). The DINAG and DINAGZ are two digestibility criteria first proposed by
178 Argillier et al. (1995). The silage traits were predicted using Near Infrared Reflectance Spectrometry (NIRS)
179 measured in the lab on silage powders or directly on fields during the harvest, depending on the trial.

180 Outlier observations were detected by examining raw data and considering field observations. They were
181 treated as missing data. Subsequently, filters were applied to identify plots with standing counts below 80% of the
182 median, and DMC below 25% or above 45%, which were also considered as missing data. Values of DINAG,
183 DINAGZ, and MFU measured in two trials were inconsistent with those of other trials and were excluded from
184 further analyses. Following quality control and filters, the percentage of missing data across all traits was 8%.

185 **Genotyping**

186 The founder lines and the G0 parental lines were genotyped for 18,480 SNPs using a proprietary Affymetrix®
187 array provided by Limagrain. The G1 parental lines were genotyped using a custom-made chip comprising a subset
188 of 15,000 SNPs of the Illumina® MaizeSNP50 BeadChip (Ganal et al. 2011). Filters were applied for both G0 and
189 G1 lines: markers with more than 20% of missing values within the dent and flint parental lines, markers with
190 more than 5% of heterozygosity among the dent (flint) parental lines, and with Minor Allele Frequency (MAF)

191 inferior to 5% were discarded. After quality control, only markers common to the two arrays were considered.
 192 4,812 SNP polymorphic markers (in at least the flint or dent population) were retained for further analyses.

193 Estimation of variance components and trait heritabilities

194 Variance components and trait heritabilities were estimated in the (G0S+G1)_F-1H design. Individual single-plot
 195 performances were corrected by the BLUPs of spatial effects predicted using the model defined in supplementary
 196 material **File S1**. Corrected data were then used to estimate variance components using the following model :

$$197 \quad Y_{hii'jl} = \mu + \lambda_l + (\tau_h + \rho_{lh}) \times t_h + [\pi_j + H_{h(ii')j} + H\lambda_{lh(ii')j}] \times (1 - t_h) + E_{hii'jl}, \quad (1)$$

198 where $Y_{hii'jl}$ is the phenotypic value corrected by spatial effects of hybrid h of generation j produced by crossing
 199 the flint parental line i and the dent parent line i' evaluated in trial l . μ is the intercept, λ_l is the fixed effect of trial
 200 l , t_h is an indicator function that distinguishes experimental hybrids (set to 0) from control hybrids (set to 1), τ_h
 201 is the fixed effect of control hybrids with 19 levels (2 for commercial hybrids + 16 for founder hybrids + one for
 202 non-control hybrids), ρ_{lh} is the effect of the interaction between trial l and control hybrid h , π_j is the fixed effect
 203 of the generation with two levels (G0S or G1 hybrids). $H_{h(ii')j}$ is the random genetic effect of experimental hybrid
 204 h of generation j , produced by crossing the flint line i and the dent line i' . $H_{h(ii')j}$ is decomposed into its GCA
 205 and SCA components as follows:

$$206 \quad H_{h(ii')j} = U_{ij} + U'_{i'j} + S_{iij}$$

207 where U_{ij} (respectively $U'_{i'j}$) is the random GCA effect of the flint line i (respectively dent line i') of generation
 208 j . We assume that U_{ij} and $U'_{i'j}$ are independent and identically distributed (iid) within generation and follow a
 209 normal distribution: $U_{ij} \sim \mathcal{N}\left(0, \sigma_{GCA_f^j}^2\right)$ and $U'_{i'j} \sim \mathcal{N}\left(0, \sigma_{GCA_d^j}^2\right)$, respectively. $\sigma_{GCA_f^j}^2$ and $\sigma_{GCA_d^j}^2$ are the flint and
 210 dent GCA variances of generation j . S_{iij} is the random SCA effect of the interaction between the parental lines i
 211 and i' , with $S_{iij} \sim \mathcal{N}\left(0, \sigma_{SCA^j}^2\right)$ and with $\sigma_{SCA^j}^2$ being the SCA variance at generation j . $H\lambda_{lh(ii')j}$ is the genotype by
 212 trial interaction and is decomposed as follows:

$$213 \quad H\lambda_{lh(ii')j} = (U\lambda)_{ij} + (U'\lambda)_{i'lj} + (S\lambda)_{iilj},$$

214 where $(U\lambda)_{ij}$ and $(U'\lambda)_{i'lj}$ are the random effects of the flint GCA effect by trial interaction, respectively dent
 215 GCA by trial interaction of generation j and $(S\lambda)_{iilj}$ is the random effect of the SCA by trial interaction of
 216 generation j . With $(U\lambda)_{ij} \sim \mathcal{N}\left(0, \sigma_{GCA \times E_f^j}^2\right)$, $(U'\lambda)_{i'lj} \sim \mathcal{N}\left(0, \sigma_{GCA \times E_d^j}^2\right)$ and $(S\lambda)_{iilj} \sim \mathcal{N}\left(0, \sigma_{SCA \times E^j}^2\right)$.

217 $\sigma_{GCA \times E_f^j}^2$, $\sigma_{GCA \times E_d^j}^2$ and $\sigma_{SCA \times E^j}^2$ are the flint GCA by trial interaction variance, the dent GCA by trial variance and
 218 the SCA by trial interaction variance of generation j , respectively. $E_{hii'jl}$ is the error term; we assume that the
 219 errors follow: $E_{hii'jl} \sim \mathcal{N}(0, \sigma_{E_l}^2)$ and are iid within trial and independent between trials, $\sigma_{E_l}^2$ is the error variance
 220 of trial l . The different random effects of the model are assumed to be independent.

221 For each trait and each generation j (G0S or G1), the percentage of genetic variance due to SCA was
 222 estimated (%), and broad-sense heritability was computed as follows:

$$223 \quad H_j^2 = \frac{\sigma_{H_j}^2}{\sigma_{H_j}^2 + \frac{\sigma_{H \times E_j}^2}{n_{site}} + \frac{\sigma_{E_{moy}}^2}{n_{rep} \times n_{site}}},$$

224 where $\sigma_{H_j}^2$ is the hybrid genetic variance of generation j computed as $\sigma_{H_j}^2 = \sigma_{GCA_f^j}^2 + \sigma_{GCA_d^j}^2 + \sigma_{SCA^j}^2$, $\sigma_{H \times E_j}^2$ is the
 225 total genotype by trial variance of generation j decomposed as: $\sigma_{H \times E_j}^2 = \sigma_{GCA \times E_f^j}^2 + \sigma_{GCA \times E_d^j}^2 + \sigma_{SCA \times E^j}^2$, and $\sigma_{E_{moy}}^2$
 226 is the mean residual variance across all trials, n_{site} is the average number of trials in which an hybrid has been
 227 evaluated and n_{rep} is the average number of within trial replicates per hybrid across trials.

228 **LS-means and genetic gain estimation**

229 Least square-means (ls-means) of hybrids were computed over the eight trials. The model used was:

$$230 \quad Y_{hrl}^* = \mu + \lambda_l + \gamma_h + E_{hrl} \quad (2)$$

231 In this model, experimental hybrids and founder hybrids were considered jointly. Y_{hrl}^* is the performance corrected
 232 by the spatial field effects of repetition r of hybrid h in trial l . μ is the intercept, λ_l is the fixed effect of trial l , γ_h
 233 is the fixed genetic effect of hybrid h . E_{hrl} is the error term of environment l , with $E_{hrl} \sim \mathcal{N}(0, \sigma_{E_l}^2)$ iid within trial
 234 and independent between trials. All genomic predictions were performed on the ls-means thus obtained.

235 The founder hybrids were used as a reference for the initial unselected population. The observed genetic
 236 gain was computed as the difference between the performances of the founder hybrids and the experimental
 237 hybrids (either the G0S or the G1 hybrids). Then, we compared the observed to the predicted genetic gain estimated
 238 from the genomic predictions of hybrid values trained on the G0_F-1H.

239 **Pedigree based Best Linear Unbiased Prediction (PBLUP) model**

240 A prediction model based on the pedigree information (PBLUP) model was implemented and used as a benchmark
 241 compared to the GBLUP models. The model was:

242
$$\mathbf{y} = \mathbf{1}_n \cdot \mu + \mathbf{Z}\mathbf{g} + \mathbf{E}, (3)$$

243 where \mathbf{y} is the vector of ls-means of the n phenotyped hybrids, $\mathbf{1}_n$ is a vector of n ones and μ is the intercept. \mathbf{g} is
 244 the vector of random hybrid effects, with $\mathbf{g} \sim \mathcal{N}(0, \mathbf{K}\sigma_h^2)$ where \mathbf{K} is the pedigree kinship matrix computed on the
 245 hybrid population considering the founder lines as the base generation. The pedigree kinship matrix was computed
 246 with the recursive method presented in Mrode and Thompson (2005) using the AHGmatrix R-package (Amadeu
 247 et al. 2016). σ_h^2 is the hybrid variance. \mathbf{Z} is the corresponding incidence matrix. \mathbf{E} is the vector of error terms, with
 248 $\mathbf{E} \sim \mathcal{N}(0, \mathbf{I}\sigma_E^2)$. The random effects are assumed to be independent.

249 **Genomic Best Linear Unbiased Prediction (GBLUP) models**

250 Several GBLUP models were tested to evaluate the predictive ability within the G1 cycle. Two types of models
 251 can be distinguished: the GCA-models, which decompose the hybrid genetic effect into its parental GCAs and its
 252 SCA components and the G-models, which consider genetic effects defined based on the hybrid marker genotypes.

253 **GCA.1-model.** Two GBLUP models were implemented for genomic predictions depending on the TRS design
 254 (factorial or tester). The model implemented on the factorial designs including SCA effects was:

255
$$\mathbf{y} = \mathbf{1}_n \cdot \mu + \mathbf{Z}_d \mathbf{g}_{GCA_d} + \mathbf{Z}_f \mathbf{g}_{GCA_f} + \mathbf{Z} \mathbf{g}_{SCA_{df}} + \mathbf{E}, (4.1)$$

256 where \mathbf{y} is the vector of ls-means of the n phenotyped hybrids, $\mathbf{1}_n$ is a vector of n ones and μ is the intercept.
 257 \mathbf{g}_{GCA_f} (respectively \mathbf{g}_{GCA_d}) is the vector of random GCA effects of the n_f flint parental lines (respectively n_d dent
 258 lines), with $\mathbf{g}_{GCA_f} \sim \mathcal{N}(0, \mathbf{K}_{GCA_f} \sigma_{GCA_f}^2)$ (respectively $\mathbf{g}_{GCA_d} \sim \mathcal{N}(0, \mathbf{K}_{GCA_d} \sigma_{GCA_d}^2)$) where \mathbf{K}_{GCA_f} (respectively
 259 \mathbf{K}_{GCA_d}) is the genomic relatedness matrix between the flint lines (respectively dent lines). The kinship matrix was
 260 computed for all the flint (dent) parental lines following method 1 from VanRaden (2008). $\sigma_{GCA_f}^2$ and $\sigma_{GCA_d}^2$ are
 261 the flint and dent GCA variances. $\mathbf{g}_{SCA_{df}}$ is the vector of SCA random effects of the n hybrids, accounting for the
 262 interactions between the flint and dent parental lines, with $\mathbf{g}_{SCA_{df}} \sim \mathcal{N}(0, \mathbf{K}_{SCA_{df}} \sigma_{SCA_{df}}^2)$ where $\mathbf{K}_{SCA_{df}}$ is the
 263 SCA kinship matrix of the hybrids (phenotyped or not) and $\sigma_{SCA_{df}}^2$ the SCA variance. The coefficient of the SCA
 264 kinship between two flint-dent hybrids produced from crossing parental lines i to j and parental lines i' to j' were
 265 computed as the product between the flint GCA kinship coefficient between lines i and i' and the dent GCA
 266 kinship coefficient between lines j and j' (Stuber and Cockerham 1966). \mathbf{Z}_d , \mathbf{Z}_f and \mathbf{Z} are the corresponding
 267 incidence matrices. \mathbf{E} is the vector of error terms, with $\mathbf{E} \sim \mathcal{N}(0, \mathbf{I}\sigma_E^2)$. The different random effects are assumed
 268 to be independent.

269 The model implemented on the G0_T-F was:

$$270 \quad \mathbf{y} = \mathbf{1}_n \cdot \mu + \mathbf{X}\mathbf{v} + \mathbf{Z}_f \mathbf{g}_{GCA_f} + \mathbf{Z} \mathbf{g}_{SCAt} + \mathbf{E}, \quad (4.2)$$

271 where \mathbf{y} is the vector of ls-means of the n phenotyped hybrids, $\mathbf{1}_n$ is a vector of n ones and μ is the intercept. \mathbf{v} is
 272 the vector of fixed effects of the two dent testers. \mathbf{g}_{GCA_f} is the vector of random GCA effects of the n_f flint parental
 273 lines, with $\mathbf{g}_{GCA_f} \sim \mathcal{N}\left(0, \mathbf{K}_{GCA_f} \sigma_{GCA_f}^2\right)$ where \mathbf{K}_{GCA_f} is the genomic relatedness matrix between the flint lines and
 274 $\sigma_{GCA_f}^2$ is the flint GCA variance. \mathbf{g}_{SCAt} is the vector of random effects of the interaction between the flint line and
 275 the dent testers, with $\mathbf{g}_{SCAt} \sim \mathcal{N}\left(0, \mathbf{I}_2 \otimes \mathbf{K}_{GCA_f} \sigma_{SCAt}^2\right)$ where σ_{SCAt}^2 is the SCA variance. The kinship matrix was
 276 computed for all the flint parental lines following method 1 from VanRaden (2008). \mathbf{X} , \mathbf{Z}_f and \mathbf{Z} are the
 277 corresponding incidence matrices. \mathbf{E} is the vector of error terms, with $\mathbf{E} \sim \mathcal{N}\left(0, \mathbf{I} \sigma_E^2\right)$. The different random effects
 278 are assumed to be independent. The same model was adapted and implemented on the G0_T-D.

279 **GCA.2-model.** This GCA-model was defined following González-Diéguez et al. (2021), where the
 280 genetic effect is defined according to gamete origin. The fullest model for the factorial TRS was:

$$281 \quad \mathbf{y} = \mathbf{1}_n \cdot \mu + \mathbf{Z}_d \mathbf{g}_{A_d} + \mathbf{Z}_f \mathbf{g}_{A_f} + \mathbf{Z} \mathbf{g}_D + \mathbf{Z}_d \mathbf{g}_{AA_d} + \mathbf{Z}_f \mathbf{g}_{AA_f} + \mathbf{Z} \mathbf{g}_{AA_{df}} + \mathbf{E}, \quad (6)$$

282 where \mathbf{y} is the vector of ls-means of the n phenotyped hybrids, $\mathbf{1}_n$ is a vector of n ones and μ is the intercept. \mathbf{g}_{A_f}
 283 and \mathbf{g}_{A_d} are the vectors of the random additive effect from the flint and dent parental lines with
 284 $\mathbf{g}_{A_f} \sim \mathcal{N}\left(0, \mathbf{K}_{A_f} \sigma_{A_f}^2\right)$ and $\mathbf{g}_{A_d} \sim \mathcal{N}\left(0, \mathbf{K}_{A_d} \sigma_{A_d}^2\right)$, respectively. \mathbf{g}_D is the vector of random dominance effect with
 285 $\mathbf{g}_D \sim \mathcal{N}\left(0, \mathbf{K}_D \sigma_D^2\right)$, \mathbf{g}_{AA_f} is the vector of random additive-by-additive epistatic effect within the flint (resp. dent)
 286 population with $\mathbf{g}_{AA_f} \sim \mathcal{N}\left(0, \mathbf{K}_{AA_f} \sigma_{AA_f}^2\right)$ (resp. $\mathbf{g}_{AA_d} \sim \mathcal{N}\left(0, \mathbf{K}_{AA_d} \sigma_{AA_d}^2\right)$) and $\mathbf{g}_{AA_{df}}$ is the vector of random
 287 additive-by-additive epistatic effect across the flint and dent populations $\mathbf{g}_{AA_{df}} \sim \mathcal{N}\left(0, \mathbf{K}_{AA_{df}} \sigma_{AA_{df}}^2\right)$. \mathbf{K}_{A_f} , \mathbf{K}_{A_d} ,
 288 \mathbf{K}_D , \mathbf{K}_{AA_f} , \mathbf{K}_{AA_d} and $\mathbf{K}_{AA_{df}}$ are respectively the flint additive, dent additive, dominance, additive-by-additive
 289 epistasis within the flint population, additive-by-additive epistasis within the dent population and the additive-by-
 290 additive epistasis across populations genomic relatedness matrices computed following González-Diéguez et al.
 291 2021. $\sigma_{A_f}^2$, $\sigma_{A_d}^2$, σ_D^2 , $\sigma_{AA_f}^2$, $\sigma_{AA_d}^2$ and $\sigma_{AA_{df}}^2$ are the corresponding variances. \mathbf{Z}_f , \mathbf{Z}_d and \mathbf{Z} are the incidence
 292 matrices. \mathbf{E} is the vector of error terms, with $\mathbf{E} \sim \mathcal{N}\left(0, \mathbf{I} \sigma_E^2\right)$. The different random effects are assumed to be
 293 independent.

294 **G-model.** This model was defined by Vitezica et al. (2017). It is based on the hybrid genotypes and does
 295 not account for the gamete origin (flint and dent parental origins). The fullest model considered for the factorial
 296 TRS was:

$$297 \quad \mathbf{y} = \mathbf{1}_n \cdot \mu + \mathbf{Z}\mathbf{g}_A + \mathbf{Z}\mathbf{g}_D + \mathbf{Z}\mathbf{g}_{AA} + \mathbf{E}, (5)$$

298 where \mathbf{y} is the vector of ls-means of the n phenotyped hybrids, $\mathbf{1}_n$ is a vector of n ones and μ is the intercept. \mathbf{g}_A
 299 is the vector of the random additive effect with $\mathbf{g}_A \sim \mathcal{N}(0, \mathbf{K}_A \sigma_A^2)$, \mathbf{g}_D is the vector of random dominance effect
 300 with $\mathbf{g}_D \sim \mathcal{N}(0, \mathbf{K}_D \sigma_D^2)$ and \mathbf{g}_{AA} is the vector of random additive-by-additive epistasis effect with
 301 $\mathbf{g}_{AA} \sim \mathcal{N}(0, \mathbf{K}_{AA} \sigma_{AA}^2)$. \mathbf{K}_A , \mathbf{K}_D and \mathbf{K}_{AA} are respectively the additive, dominance and additive-by-additive
 302 epistasis genomic relatedness matrices computed following Vitezica et al. 2017. σ_A^2 , σ_D^2 and σ_{AA}^2 are the
 303 corresponding variances and \mathbf{Z} is the incidence matrix. \mathbf{E} is the vector of error terms, with $\mathbf{E} \sim \mathcal{N}(0, \mathbf{I}\sigma_E^2)$. The
 304 different random effects are assumed to be independent.

305 **Prediction scenarios**

306 We defined three prediction scenarios to achieve three objectives: (i) assess the predictive ability of GS
 307 in the new generation and compare different GS models, (ii) evaluate the efficiency of a factorial design for
 308 predictions across breeding cycles and compare it to the tester designs, and n (iii) investigate the benefit of different
 309 strategies to update the factorial TRS across cycles and optimize it using the CDmean to predict the new generation.

310 In Scenario 1, we evaluated the predictive ability within the new generation (G1 hybrids) to serve as a
 311 reference and compared the efficiency of several GS models. Cross-validations within the G1 hybrids were
 312 performed by training the GS model on 354 G1 hybrids (four-fifth) to predict the remaining 88 G1 hybrids (one-
 313 fifth). This process was repeated a hundred times. We compared three types of GBLUP models, namely the
 314 GCA.1-model, G-model, and GCA.2-model, to a benchmark PBLUP model. The GCA.1-model involved two
 315 nested models, with or without the SCA effect. For the GCA.2- and G-models, several nested models were tested
 316 by adding successively dominance and additive-by-additive genetic effects to additive effects. See **Table 2** for the
 317 summary of all tested models.

318 Scenario 2 evaluated the efficiency of training a GBLUP model (GCA.1) on the G0 generation to predict
 319 the next one (G1). In Scenario 2a, we evaluated the efficiency of the incomplete factorial TRS (G0_F-1H) to
 320 predict G1 hybrids. We assessed the prediction stability across breeding cycles by comparing the predictive
 321 abilities obtained for the G1 hybrids to the one obtained for the G0S hybrids evaluated in the same experiments.

322 The GCA.1 model was used to perform predictions. In Scenario 2b, we compared the efficiency of factorial and
323 tester TRSs from the G0 cycle to predict the G1 cycle. The GCA.1 models (4.1) or (4.2) were trained on the G0_F-
324 4H (363 hybrids) or the tester designs (360 hybrids) to predict G1 hybrids. We investigated the impact of the TRS
325 on hybrid selection through the correlation between the GCA BLUPs predicted using the factorial and the ones
326 obtained using the tester designs. In addition, to compare the similarity of selection between the different
327 approaches (based on phenotypic evaluations (ls-means) or genomic predictions (BLUPs) trained on the factorial
328 or the tester designs), the coincidence of selection was computed for each trait. For each pair of approaches, it
329 corresponds to the percentage of common hybrids that would be selected by the two approaches at a given selection
330 rate (%). This coincidence of selection was computed for different selection rates. As in Lorenzi et al. 2022, we
331 sampled hybrids in the tester designs to evaluate the impact of the number of testers used in the TRS. In this
332 Scenario 2b', each tester TRS was composed of 180 hybrids produced by crossing in each group: (i) 90 lines to
333 one tester (180 lines in total): since there were two testers in each group, there were four possible tester
334 combinations, referred to as 1T-180H-180L- followed by the names of the testers, (ii) 45 lines to one tester and
335 the 45 other lines to the other tester, referred to as 2T-180H-180L, (iii) the same 45 lines to two testers referred to
336 as 2T-180H-90L. We compared these tester TRS to a factorial TRS by sampling 180 hybrids from the G0_F-4H
337 in a random and balanced manner between families to maximize the number of lines. This factorial TRS comprised
338 180 hybrids representing 170 lines (one line contributed to 2.1 hybrids on average) and was called F-180H-170L.
339 In Scenario 2b', all the TRSs were sampled ten times except for the one-tester designs that were sampled only
340 once.

341 Scenario 3 investigated TRS optimization across breeding cycles. In Scenario 3a, we evaluated the benefit
342 of updating the TRS across cycles by adding either G0S or/and G1 hybrids to the initial G0R TRS. Several TRSs
343 were sampled and compared to cross-validations within the G1 hybrids. To assess the benefit of adding G0S
344 hybrids to the initial G0R TRS, we compared TRSs only composed of G0R hybrids with the same TRSs to which
345 132 G0S hybrids from the G0_F-4H design were added. To evaluate the benefit of updating G0 TRSs with G1
346 hybrids, we added from 0 to 354 randomly sampled G1 hybrids to G0 TRSs. One-fifth of the G1 hybrids (88
347 hybrids) were predicted using the GCA.1 model. The mean predictive ability over 100 replicates was computed
348 for each TRS. In Scenario 3b, our objective was to maximize the predictive ability of the G1 hybrids by optimizing
349 *a priori* the G1 hybrid subset used to update the initial G0 TRS using only G1 line genotypes. We considered the
350 CDmean proposed by Rincent et al. (2012). We used a heritability of 0.7, corresponding to the average heritability
351 of our traits, to compute the value for the shrinkage parameter λ and the additive covariance kinship between

352 hybrids defined by Vitezica et al. (2017). Two optimization strategies were considered and compared to random
353 sampling. For both strategies, we optimized the mean of the CD of contrasts between each non-phenotyped G1
354 hybrid (PS) and the mean of the G1 hybrids. In the first strategy (CDmean1), the G1 hybrid set was optimized
355 without considering the marker information on the G0 hybrids. The additive kinship considered to compute
356 expected CDmeans only included the 442 G1 hybrids. In the second strategy (CDmean2), the optimization of the
357 G1 was performed by also considering information on the G0 hybrids: the additive kinship was computed for all
358 1802 hybrids from both generations (1360 G0+ 442 G1). The procedure was performed in both scenarios with four
359 sampling sizes for the G1 hybrids (50,100, 200, and 300) and replicated a hundred times each. For each optimized
360 set, all G0 hybrids plus the chosen G1 hybrids were used as TRS to predict the remaining G1 hybrids, used as VS.
361 Predictions were performed using the GCA.1 model.

362 **Predictive ability and statistical tests**

363 In all scenarios, the predictive ability was computed as Pearson's correlation between predicted hybrid values and
364 hybrid ls-means. Different statistical tests were performed depending on the scenario to test the significance of
365 differences between predictive abilities. In Scenario 1, paired t-tests were performed with a risk level $\alpha=0.05$, and
366 a Bonferroni correction (multiple comparison correction) was applied per trait. In Scenario 2b, Williams tests
367 (Williams 1959) were performed with a risk level $\alpha=0.05$ using the "r.test" function of the psych R-package
368 (Revelle 2021). In Scenario 2b', t-tests with a risk level $\alpha=0.05$ were performed, and a Bonferroni correction was
369 applied per trait. For all scenarios, computations were performed in the R statistical environment (R Core Team
370 2020), and models were fitted using the "MM4LMM" R-package (Laporte and Mary-Huard 2020; Laporte et al.
371 2022).

372 **Results**

373 For clarity purposes, results on the four main traits of interest (DMY, DMC, DtSilk, and MFU) are presented in
374 the following. The results on the 11 studied traits are shown in supplementary materials.

375 **Variance components and broad-sense heritability (H^2) at the phenotypic level without marker information**

376 Broad-sense heritabilities (H^2) were medium to high (**Table 3**). They ranged from 0.56 (MFU) to 0.93 (DtSilk) for
377 G0S hybrids and from 0.62 (MFU) to 0.94 (DtSilk) for G1 hybrids. Large and significant genetic variances were
378 observed for all traits (**Table 3, Table S1**) with no clear differences between G0S and G1 hybrids. The main part
379 of the genetic variance was due to GCA. The proportion of genetic variance due to SCA ranged from 0% (DMC)

380 to 30% (MFU) for the G0S and from 0% (DMY) to 10% (DMC) for the G1. σ_{GCAf}^2 was always larger than σ_{GCAd}^2
381 except for G0S hybrids for DMC. Non-null GCA by trial variances were observed for G0S and G1 hybrids, but
382 were lower than the GCA variances. For the G0S, σ_{SCA}^2 was larger than σ_{SCAxE}^2 for all traits. For G1 hybrids, σ_{SCAxE}^2
383 was larger than σ_{SCA}^2 , except for DtSilk.

384 **Ls-means and genetic gain**

385 On average, G0S and G1 hybrids performed similarly (**Table 4**). Compared to the 16 founder hybrids, which are
386 representative of the performance of the unselected G0 hybrids (G0R), G0S and G1 hybrids showed a gain in
387 performance for DMY (+1.55 t/ha for G0S and +1.52 t/ha for G1). This gain was associated with a later DtSilk
388 (+1.83 days for G0S and +1.90 days for G1), a lower DMC (-0.77% for G0S and -0.67% for G1), and a lower
389 MFU (-2.11 MFUx10²/kg for G0S and -2.15 MFUx10²/kg for G1). The observed genetic gain for DMY was similar
390 to the predicted one based on the genomic predictions trained on the G0_F-1H design. However, for DMC, DtSilk,
391 and MFU, the observed response to selection was higher in absolute value than the predicted one.

392 **Scenario 1- Predictive ability within the G1 cycle and GS model comparison**

393 We assessed the predictive ability in the new breeding cycle using cross-validations among G1 hybrids (**Fig.2**).
394 GBLUP predictive abilities of the new generation were high for all traits, ranging from 0.63 (DMY) to 0.76
395 (DtSilk) when considering the best GBLUP model. All GBLUP models significantly outperformed the PBLUP
396 model (differences between the worst GBLUP model and the PBLUP ranged from 0.07 (DMY) to 0.11 (MFU)).
397 Differences among GBLUP models were sometimes significant but minor (<0.01), showing that models were
398 equivalent and that adding non-additive effects had little effect.

399 **Scenario 2- Efficiency of a factorial TRS for predictions across breeding cycles and comparison with tester**

400 **TRSs**

401 In Scenario 2a, we compared the ability of the G0_F-1H TRS to predict the same generation (G0S hybrids) or the
402 new generation (G1 hybrids). Predictive abilities were high for all traits (ranging from 0.56 for DMY to 0.67 for
403 DtSilk for G1 hybrids and from 0.60 for DMY to 0.75 for MFU for G0S hybrids) (**Fig. 3**). As expected, predictive
404 abilities were higher for G0S hybrids (hybrids from the same generation as the TRS hybrids) than for G1 hybrids
405 for all traits. Lower predictive abilities were obtained when training on the G0_F-1H compared to those obtained
406 by cross-validations within G1 hybrids (**Fig. 3**).

407 In Scenario 2b, we compared predictive abilities obtained using either the G0_F-4H (363 hybrids) or the
408 G0 tester designs (360 hybrids) as TRS to predict all G1 hybrids (442 hybrids) (**Fig. 4**). They ranged from 0.59
409 (DMY and MFU) to 0.70 (DtSilk) when training on the G0_F-4H and from 0.60 (MFU) to 0.69 (DtSilk) when
410 training on the G0 tester designs. Across the 11 traits, training on the G0_F-4H or the G0 tester designs gave
411 equivalent predictive abilities except for four traits: the G0_F-4H design significantly outperformed the G0 tester
412 designs for DMC and PH, and the G0 tester designs significantly outperformed the G0_F-4H design for DMY and
413 CELL (**Fig. S1**). The GCA BLUPs of the G1 lines predicted using the G0_F-4H or the G0 tester designs as TRS
414 were highly correlated. They ranged from 0.85 (DMC) to 0.94 (MFU) for the dent G1 lines and from 0.84 (DMY)
415 to 0.94 (DtSilk) for the flint G1 lines, and from 0.87 (DMY, DMC) to 0.91 (DtSilk) for G1 hybrids (**Table S4**).
416 The coincidence of selection for genomic predictions between the factorial and the tester TRS of the top 5% of
417 hybrids was 52% for DMY, 61% for DMC, 65% for DtSilk, and 39% for MFU (**Fig. S2**), which indicates that the
418 single-cross hybrid sets selected by the two approaches are not identical. To assess if one of the two approaches
419 identified a higher proportion of the best-phenotyped hybrids, we compared the proportion of the top 5% hybrids
420 identified based on the factorial or tester TRS to the top 5% phenotyped hybrids. For DMY, the major trait of
421 interest in our study, the factorial design identified a higher proportion of the best-phenotyped hybrids compared
422 to the tester designs.

423 In Scenario 2b', we investigated the efficiency of different G0 tester design compositions to predict G1
424 hybrids (442 hybrids) at the same number of hybrids (180) and compared them with a factorial design of same size
425 (**Fig. 5**). Predictive abilities varied between the four one-tester TRS ranging from 0.005 (DMC) to 0.048 (DMY),
426 and the best one-tester TRS depended on the trait. The best two-tester TRS maximized the number of evaluated
427 candidate lines by crossing more lines each to a different tester (2T-180H-180L) and usually outperformed the
428 worst one-tester TRS. The F-180H-170L factorial TRS was equivalent to or outperformed the tester TRS except
429 for DMY. On average, over the 11 traits, the F-180H-170L TRS gave the highest predictive abilities (**Fig.5, Fig.**
430 **S3**).

431 **Scenario 3a- Benefit of updating the factorial TRS across breeding cycles**

432 To evaluate the benefit of updating the TRS across breeding cycles, four TRS strategies were evaluated
433 based on their ability to predict G1 hybrids: (i) training on G0R only (G0_F-1H, G0R_F-4H or G0_F-1H+G0R_F-
434 4H), (ii) training on G0R plus 132 hybrids between G0 selected lines (G0S), (iii) training on G0R plus a subset m
435 of hybrids from the new generation (G1 hybrids), and (iv) training on G0R plus 132 G0S hybrids and m G1 hybrids,

436 with m ranging from 1 to 354 (**Fig. 6**). The four TRS strategies were also compared to cross-validations within the
437 G1 hybrids. The best G0R TRS (G0_F-1H+G0R_F-4H) was also the largest one (1183 hybrids) with predictive
438 abilities ranging from 0.69 (MFU) to 0.76 (DMC and DtSilk), which were equivalent or higher than the ones
439 obtained with a TRS composed of 354 G1 hybrids.

440 Adding 132 G0S hybrids to the initial G0R TRSs (G0_F-1H, G0R_F-4H, or G0_F-1H+G0R_F-4H)
441 increased predictive abilities (with a gain on average of 0.10 for DMY, 0.14 for DMC, 0.16 for DtSilk and 0.05
442 for MFU). The largest gain in predictive ability was observed for the G0R_F-4H TRS, which was also the smallest
443 G0R TRS (232 hybrids), with gains ranging from 0.08 (MFU) to 0.39 (DtSilk). There was always a gain in
444 predictive ability when adding G1 hybrids to the TRS, whether composed of G0R or of G0R and G0S hybrids. As
445 expected, the gain increased with the number of G1 hybrids included in TRS. Adding 354 G1 hybrids to G0R
446 TRSs, increased predictive abilities on average by 0.13 for DMY, 0.20 for DMC, 0.21 DtSilk, and 0.12 for MFU.
447 For TRSs comprising G0R and G0S hybrids, adding 354 G1 hybrids led to smaller gains (gain not exceeding 0.07
448 for MFU). The largest increase in predictive abilities when updating the TRS with G1 hybrids was obtained with
449 the smallest initial G0R TRS (G0R_F-4H). It is interesting to note that TRSs composed of G0 and 354 G1 hybrids
450 always outperformed prediction accuracies obtained with 354 G1 (cross-validations within G1), illustrating the
451 benefit of keeping information from the previous generation in the TRS.

452 From **Fig 6**, it is possible to estimate the number of G1 hybrids to add to the initial G0R TRSs to achieve
453 similar predictive abilities to the ones obtained when adding 132 G0S hybrids. For example, for DMY and the
454 G0R_F-4H initial TRS, adding 132 G0S was equivalent to adding around 170 G1 hybrids. For all initial G0R
455 TRSs, the number of G1 hybrids to include to be more efficient than 132 G0S hybrids was higher than 132 for all
456 traits except MFU.

457 **Scenario 3b- Optimization of the composition of the factorial TRS for G1 hybrid predictions**

458 The G1 hybrid set to add to the existing G0 TRS (1360 G0 hybrids) was optimized using the CDmean following
459 two strategies, and the results were compared to a TRS obtained from random sampling (**Fig. 7**). In the first strategy
460 (CDmean1), the G1 hybrid set was optimized without considering the information from the G0 hybrids, whereas
461 in the second strategy (CDmean2), the information from the G0 hybrids was considered. For all traits and all
462 sampling sizes, the best CDmean strategy gave higher or at least equivalent predictive abilities compared to random
463 sampling except for DMC for a sampling size of 300. The maximum gains were 0.03 for DMY, 0.01 for DMC,
464 0.03 for DtSilk, and 0.02 for MFU, depending on the sampling size. Across the 100 replicates, the variance of the

465 predictive abilities was always lower using the CDmean (1 or 2) than the random sampling. The CDmean1, which
466 does not consider G0 hybrid information to optimize the G1 hybrid set included in the TRS, outperformed the
467 CDmean2 except for small sampling sizes (size 50 and 100 for DMY, size 50 for DMC, DtSilk, and MFU).

468 **Discussion**

469 **SCA variance and its importance in hybrid breeding**

470 The SCA variance estimated in the G1 generation was small or equal to zero (**Table 3, Table S2**). Small SCA
471 variance was expected in hybrids produced by crossing lines from divergent populations (Reif et al. 2007). The
472 estimated SCA percentage decreased for all traits from G0 to G1 hybrids (**Table S3**). The precision of SCA
473 variance estimation in our experiment is limited and does not allow us to draw a final conclusion on this evolution.
474 However, one possible explanation for the decrease in SCA variance we observed is that the recurrent reciprocal
475 selection increased the divergence between groups (as also observed by Gerke et al. (2015)) and, as a result,
476 decreased the SCA variance in the flint-dent single-cross hybrids (consistent with theoretical expectations from
477 Reif et al. (2007) and Legarra et al. (2023)).

478 **Genetic gain after selection based on genomic predictions trained on a sparse factorial design**

479 The population was selected for an index combining yield performance (DMY), dry matter content (DMC), and
480 digestibility (MFU) based on genomic predictions. We successfully improved the mean performance of the new
481 generation for DMY, but there was a decrease for MFU and DMC (**Table 4**), which was higher than expected.
482 The negative correlation (-0.53) between DMY and MFU that was observed based on phenotypic data in the G0
483 generation (G0_F-1H) (**Fig. S4**) certainly explains the difficulty of improving both traits simultaneously. This was
484 consistent with results found by Barrière and Emile (2000) and Surault et al. (2005), who also reported a negative
485 correlation of -0.5 between these traits for maize silage. To maintain a stable level of DMC and improve MFU in
486 the new generation, higher weights relative to DMY should have been put on these traits in the index calculation.

487 The genetic gain predicted by the GBLUP model trained on the G0_F-1H design was similar to the
488 observed genetic gain for DMY. This illustrates the efficiency of GS models in predicting GCA values based on a
489 sparse factorial TRS and confirms the results found by Seye et al. (2020) using simulations and Lorenzi et al.
490 (2022) on the G0 generation.

491 **Predictive ability in the new generation and comparison of different GS models**

492 In Scenario 1, we evaluated the predictive ability within G1 hybrids and compared different prediction models.
493 All models gave high predictive abilities, with the lowest reaching 0.66 (for DtSilk with the PBLUP model). The
494 high predictive ability of the PBLUP model indicates that family structure alone could predict part of hybrid
495 performances. However, GBLUP models always outperformed the PBLUP, confirming the efficiency of GBLUP
496 to predict the mendelian sampling within a family, which is of main interest for breeding. Different GBLUP models
497 were tested. Differences were sometimes significant but always small (<0.01). Including non-additive genetic
498 effects had little or no effect on predictive abilities, which was also reported in studies using data from inter-
499 heterotic group hybrids (Bernardo 1994; Schrag et al. 2006, 2018; Maenhout et al. 2010; Vitezica et al. 2017;
500 González-Diéguez et al. 2021; Lorenzi et al. 2022). Note that the new SCA kinship formula proposed by González-
501 Diéguez et al. (2021) used in model GCA.2 did not improve predictive abilities compared to the one used in the
502 GCA.1 model. This was also observed by Lorenzi et al. (2022) for genomic predictions within the G0 generation.
503 In their simulations, Seye et al. (2020) found an advantage of including SCA in prediction models when SCA
504 explains about 23% of the genetic variance. The small SCA variances estimated in our experimental design are
505 consistent with the fact that including non-additive effects did not improve prediction accuracies.

506 Assuming a single additive hybrid genetic effect (G models) or additive genetic effects defined according
507 to the allele origin (GCA models) was equivalent in terms of quality of prediction for hybrid performance. This
508 was surprising considering the large differences in GCA variances observed between the two groups and the
509 detection of group-specific QTLs in the G0_F-1H design (Giraud et al. 2017b). The equivalence in terms of
510 prediction accuracy between the G and GCA models was also shown in hybrid populations by Technow et al.
511 (2014), González-Diéguez et al. (2021), and Alves et al. (2019). Even if the GCA model did not outperform the G
512 model, it makes it possible to estimate parental line values and thus select the parental lines of the next cycle,
513 which is less straightforward with a G model. We kept the GCA.1 model for the following genomic prediction
514 scenarios for these reasons.

515 **Portability of genomic predictions trained on a sparse factorial across breeding cycles**

516 In Scenario 2a, we trained the GS model on the G0_F-1H to predict G0S and G1 hybrids, allowing us to
517 evaluate the predictive ability across cycles and environments. We obtained high predictive abilities for G0S
518 hybrids, which illustrates the ability of the GS model trained on the G0_F-1H design to predict the performances
519 of a new set of hybrids between selected lines in new environments. This confirms previous results (Lorenzi et al.

520 2022), which considered another set of G0S hybrids evaluated in the 2016-2017 G0_F-4H trials. We observed
521 lower predictive abilities for G1 compared to G0S hybrids. Note that G0S and G1 hybrids were evaluated in the
522 same environments, therefore, the decrease in predictive ability is not attributable to an environmental effect. A
523 decrease in prediction accuracy when generations differ between the TRS and PS was reported in simulations
524 (Pszczola and Calus 2016; Seye et al. 2020) and experimental studies on hybrids (on sugar beet by Hofheinz et al.
525 2012; on barley Sallam et al. 2015 and Michel et al. 2016 and on maize by Wang et al. 2020). This decrease is
526 expected as selection modifies allele frequencies along generations, and recombination events modify marker-
527 QTL linkage disequilibrium. Allelic frequencies are identical in G0S and G1 hybrids since G1 lines are the
528 unselected progeny of G0S lines. Thus, the observed decrease is due to the recombination events. Still, predictive
529 abilities remained high, highlighting the efficiency of the GS model trained on the G0_F-1H design in decorrelating
530 the contributions from each parental line to predict their GCAs, the GCAs of their progeny, and therefore the
531 hybrid values across breeding cycles.

532 **Efficiency of factorial compared to tester TRSs for predictions across the breeding cycle**

533 In Scenario 2b, we compared, for the same number of hybrids and lines, the efficiency of the factorial and tester
534 TRSs to predict hybrids across generations. A previous study using the same TRSs to predict the G0 generation
535 showed slightly higher predictive abilities using the factorial compared to the tester TRSs (Lorenzi et al. 2022).
536 This advantage decreased when predicting the new generation (G1). This is in accordance with results from
537 simulations based on a similar design (Seye et al. 2020), which showed that the advantage of the factorial over the
538 tester TRSs decreases across breeding cycles if the TRS was not updated. When investigating several tester designs
539 composition (Scenario 2b'), we showed that the best strategy was always to use more testers while maximizing
540 the number of candidate lines, a strategy comparable to using a sparse factorial design.

541 **Benefit of updating the factorial TRS along breeding cycles**

542 Once inbred lines from a new generation (G1) are available and can be genotyped, a key issue is to predict the best
543 new hybrid combinations between them to prioritize hybrid production and evaluation. There are two possible
544 situations, depending on the availability of phenotypes of a subset of hybrids from the new breeding cycle (G1
545 hybrids). When G1 phenotypes are available, they can be used to calibrate prediction equations. We showed the
546 benefit of combining this information with historical data from G0 hybrids compared to using G1 phenotypes
547 alone (**Fig.6**). Several studies also reported similar results (Jannink 2010; Denis and Bouvet 2013; Neyhart et al.
548 2017). Among the historical data, hybrids between the lines selected to generate the new generation (G0S) are the

549 most related to the G1 generation. We showed that even when G0S and G1 hybrids were already in the TRS, there
550 was still a benefit of including hybrids between unselected lines from previous generations (G0R hybrids). This
551 last result aligns with results found by Neyhart et al. (2017) and Brandariz and Bernardo (2018), showing that
552 when constructing a TRS, one must consider keeping hybrids produced between unselected lines to maintain high
553 prediction accuracy. Additionally, when including data from the two generations (G0 and G1) in the TRS, we also
554 included TRS hybrids evaluated in different years and environments. This reduced the impact of genotype-by-
555 environment interactions and, as a result, increased prediction accuracy. Similar results have been obtained by
556 Auinger et al. (2016).

557 In the second situation, where G1 hybrids phenotypes are not yet available, we showed that using only
558 historical data in the TRS can provide good prediction accuracies (**Fig.6**). We evaluated the benefit of producing
559 and phenotyping additional data to update the historical (G0) TRS, particularly the benefit of adding G0S hybrids.
560 G0S are single-crosses between the G0 lines selected to be the parents of the G1 generation, so including these
561 hybrids increases the relationship between the TRS and the G1 PS. We compared G0S and G1 hybrids for their
562 efficiency to update the TRS. Predictive abilities obtained with the 132 G0S hybrids were reached when adding a
563 similar number or more G1 hybrids (**Fig.6**). This indicates that for a fixed number of hybrids, using G0S hybrids
564 was equivalent to or slightly better than using G1 hybrids for updating the TRS. Once the best candidate lines are
565 selected to become the parental lines (corresponding to G0S lines) for the subsequent breeding cycle, but hybrids
566 from the new cycle (G1 hybrids) are not yet available, it is beneficial to phenotype new hybrid combinations
567 between the selected lines to update the TRS. Several entangled factors can explain the result: (i) the increased
568 TRS size, (ii) the increased relationship between the TRS and PS, and (iii) the increased number of years and
569 environments in the data used as TRS (see reviews by Isidro y Sánchez and Akdemir 2021 and Rio et al. 2022).
570 Adding G0S hybrids is a way to accumulate information on the hybrid values (GCAs) of the selected lines in
571 different environments, which is helpful to predict the hybrid values of their progeny. Our results also show that
572 even if G0S hybrids are added to the TRS, it is still interesting to add performances of G1 hybrids to the TRS
573 when these become available, as it increases the genotypic relatedness between the TRS and the PS (**Fig.6**).

574 **Optimization of the G1 hybrid set to phenotype to update the TRS**

575 In Scenario 3b, we optimized the G1 hybrid set used to update the initial G0 TRS. The G1 hybrid set was optimized
576 based on the CDmean computed considering (CDmean 2) or not (CDmean 1) the information from the initial G0
577 TRS (G0R+G0S hybrids) (**Fig.7**). As expected, optimizing the TRS using the CDmean (CDmean 1 or CDmean 2)

578 instead of random sampling increased our predictive abilities in most of the cases. This was also reported in
579 numerous other studies (Rincent et al. 2012, 2017; Isidro et al. 2015; Akdemir et al. 2015; Mangin et al. 2019;
580 Isidro y Sánchez and Akdemir 2021; Kadam et al. 2021). Interestingly, we observed more stable predictions
581 abilities across replicates using the CDmean, than with random sampling. It has to be noted that in this optimization
582 process, we used CDs computed assuming a single additive genetic effect despite using a GCA/SCA prediction
583 model for our predictions. We could have included non-additive effects in the computation of the CDmean, as
584 done by Momen and Morota (2018) and Fristche-Neto et al. (2018). However, these authors did not find a clear
585 benefit of accounting for dominance in the CDmean computation, and we did not see any advantage of including
586 the dominance effect in our prediction models. For these reasons, we do not expect that adding dominance in the
587 CDmean computation would have had a positive impact.

588 It was surprising to us that the CDmean 1 (which does not consider information from the G0 TRS hybrids)
589 outperformed the CDmean 2 (which considers the G0 information). The CDmean 1 likely selected G1 hybrids that
590 were representative of the whole range of G1 hybrids. In contrast, since the hybrids between the G0S parental lines
591 of the G1 were already in the TRS, the CDmean 2 likely maximized the diversity of the TRS by favoring G1
592 hybrids genetically distant from the G0 hybrids. The CDmean 2 assumed that G0 and G1 hybrids were evaluated
593 in the same environments, which was not true. As a consequence, some of the G0 hybrids may not have been as
594 informative to predict the G1 hybrids as they seemed, based on the genomic relationship matrix. This may explain
595 why CDmean 2 did not outperform CDmean 1. To compute the CDmean, we could have considered each
596 environment as a different trait and used the correlation value between the two environments, as suggested by Ben-
597 Sadoun et al. (2020). Rio et al. (2022a) showed the benefit of using such multi-environmental CDs to optimize the
598 allocation of individuals in trial networks, and this could have been extended to multigeneration TRS optimization.
599 In practice, one cannot know in advance the correlation between the environments where the previous generation
600 was evaluated and those where the new generation will be evaluated. One solution might be to use historical data
601 to estimate the magnitude of correlations that can be expected between years and use this value when computing
602 the expected multi-environment CD.

603 **Conclusions**

604 Our study confirms the efficiency of combining genomic predictions and sparse factorial TRS to predict candidate
605 lines GCAs and hybrid values across breeding cycles. Genomic prediction accuracy was high and increased when
606 updating the TRS by incorporating performances of hybrids between selected lines from the previous generation

607 and potentially hybrids from the new generation. When incorporating hybrids from the new generation, choosing
608 them based on a criterion such as the CDmean was beneficial.

609 **References**

- 610 Akdemir D, Sanchez JI, Jannink J-L (2015) Optimization of genomic selection training populations with a genetic
611 algorithm. *Genet Sel Evol* 47:38. <https://doi.org/10.1186/s12711-015-0116-6>
- 612 Alves FC, Granato ÍSC, Galli G, et al (2019) Bayesian analysis and prediction of hybrid performance. *Plant*
613 *Methods* 15:14. <https://doi.org/10.1186/s13007-019-0388-x>
- 614 Amadeu RR, Cellon C, Olmstead JW, et al (2016) AGHmatrix: R Package to Construct Relationship Matrices for
615 Autotetraploid and Diploid Species: A Blueberry Example. *The Plant Genome*
616 9:plantgenome2016.01.0009. <https://doi.org/10.3835/plantgenome2016.01.0009>
- 617 Andrieu J (1995) Prédiction de la digestibilité et de la valeur énergétique du maïs fourrage à l'état frais. *INRA Prod*
618 *Anim* 8:273–274. <https://doi.org/10.20870/productions-animales.1995.8.4.4136>
- 619 Argillier O, Barrière Y, Hébert Y (1995) Genetic variation and selection criterion for digestibility traits of forage
620 maize. *Euphytica* 82:175–184. <https://doi.org/10.1007/BF00027064>
- 621 Aunger H-J, Schönleben M, Lehermeier C, et al (2016) Model training across multiple breeding cycles
622 significantly improves genomic prediction accuracy in rye (*Secale cereale* L.). *Theor Appl Genet*
623 129:2043–2053. <https://doi.org/10.1007/s00122-016-2756-5>
- 624 Barrière Y, Emile JC (2000) Le maïs fourrage. III - Evaluation et perspectives de progrès génétiques sur les
625 caractères de valeur alimentaire
- 626 Ben-Sadoun S, Rincenc R, Auzanneau J, et al (2020) Economical optimization of a breeding scheme by selective
627 phenotyping of the calibration set in a multi-trait context: application to bread making quality. *Theor Appl*
628 *Genet* 133:2197–2212. <https://doi.org/10.1007/s00122-020-03590-4>
- 629 Bernardo (1994) Prediction of Maize Single-Cross Performance Using RFLPs and Information from Related
630 Hybrids. *Crop Science* 34:20. <https://doi.org/10.2135/cropsci1994.0011183X003400010003x>
- 631 Brandariz SP, Bernardo R (2018) Maintaining the Accuracy of Genomewide Predictions when Selection Has
632 Occurred in the Training Population. *Crop Science* 58:1226–1231.
633 <https://doi.org/10.2135/cropsci2017.11.0682>
- 634 Burdo B, Leon N, Kaeppler SM (2021) Testcross vs. randomly paired single-cross progeny tests for genomic
635 prediction of new inbreds and hybrids derived from multiparent maize populations. *Crop Sci* csc2.20545.
636 <https://doi.org/10.1002/csc2.20545>
- 637 Coombes NE (2009) DiGger, a spatial design program. *Biometric Bulletin* NSW Department of Primary
638 Industries, Orange, NSW
- 639 Denis M, Bouvet J-M (2013) Efficiency of genomic selection with models including dominance effect in the
640 context of Eucalyptus breeding. *Tree Genetics & Genomes* 9:37–51. <https://doi.org/10.1007/s11295-012-0528-1>
- 642 Fernández-González J, Akdemir D, Isidro y Sánchez J (2023) A comparison of methods for training population
643 optimization in genomic selection. *Theor Appl Genet* 136:30. <https://doi.org/10.1007/s00122-023-04265-6>
- 644 6
- 645 Fristche-Neto R, Akdemir D, Jannink J-L (2018) Accuracy of genomic selection to predict maize single-crosses
646 obtained through different mating designs. *Theor Appl Genet* 131:1153–1162.
647 <https://doi.org/10.1007/s00122-018-3068-8>

- 648 Ganai MW, Durstewitz G, Polley A, et al (2011) A Large Maize (*Zea mays* L.) SNP Genotyping Array:
649 Development and Germplasm Genotyping, and Genetic Mapping to Compare with the B73 Reference
650 Genome. PLOS ONE 6:e28334. <https://doi.org/10.1371/journal.pone.0028334>
- 651 Gerke JP, Edwards JW, Guill KE, et al (2015) The Genomic Impacts of Drift and Selection for Hybrid Performance
652 in Maize. Genetics 201:1201–1211. <https://doi.org/10.1534/genetics.115.182410>
- 653 Giraud H (2016) Genetic analysis of hybrid value for silage maize in multiparental designs: QTL detection and
654 genomic selection. Thesis, Paris-Saclay
- 655 Giraud H, Bauland C, Falque M, et al (2017a) Linkage Analysis and Association Mapping QTL Detection Models
656 for Hybrids Between Multiparental Populations from Two Heterotic Groups: Application to Biomass
657 Production in Maize (*Zea mays* L.). G3 Genes|Genomes|Genetics 7:3649–3657.
658 <https://doi.org/10.1534/g3.117.300121>
- 659 Giraud H, Bauland C, Falque M, et al (2017b) Reciprocal Genetics: Identifying QTL for General and Specific
660 Combining Abilities in Hybrids Between Multiparental Populations from Two Maize (*Zea mays* L.)
661 Heterotic Groups. Genetics 207:1167–1180. <https://doi.org/10.1534/genetics.117.300305>
- 662 Goering HK, Soest PJV (1970) Forage Fiber Analyses (apparatus, Reagents, Procedures, and Some Applications).
663 U.S. Agricultural Research Service
- 664 González-Diéguez D, Legarra A, Charcosset A, et al (2021) Genomic prediction of hybrid crops allows
665 disentangling dominance and epistasis. Genetics. <https://doi.org/10.1093/genetics/iyab026>
- 666 Hallauer AR, Carena MJ, Filho JBM (2010) Quantitative Genetics in Maize Breeding. Springer Science &
667 Business Media
- 668 Henderson CR (1976) A Simple Method for Computing the Inverse of a Numerator Relationship Matrix Used in
669 Prediction of Breeding Values. Biometrics 32:69. <https://doi.org/10.2307/2529339>
- 670 Hofheinz N, Borchardt D, Weissleder K, Frisch M (2012) Genome-based prediction of test cross performance in
671 two subsequent breeding cycles. Theor Appl Genet 125:1639–1645. <https://doi.org/10.1007/s00122-012-1940-5>
- 672
- 673 Howard R, Jarquin D, Crossa J (2022) Overview of Genomic Prediction Genomic predictions (GP) Methods and
674 the Associated Assumptions on the Variance of Marker Effect, and on the Architecture of the Target
675 Trait. In: Ahmadi N, Bartholomé J (eds) Genomic Prediction of Complex Traits: Methods and Protocols.
676 Springer US, New York, NY, pp 139–156
- 677 Isidro J, Jannink J-L, Akdemir D, et al (2015) Training set optimization under population structure in genomic
678 selection. Theor Appl Genet 128:145–158. <https://doi.org/10.1007/s00122-014-2418-4>
- 679 Isidro y Sánchez J, Akdemir D (2021) Training Set Optimization for Sparse Phenotyping in Genomic Selection:
680 A Conceptual Overview. Frontiers in Plant Science 12:. <https://doi.org/10.3389/fpls.2021.715910>
- 681 Jannink J-L (2010) Dynamics of long-term genomic selection. Genetics Selection Evolution 42:35.
682 <https://doi.org/10.1186/1297-9686-42-35>
- 683 Kadam DC, Lorenz AJ (2018) Toward Redesigning Hybrid Maize Breeding Through Genomics-Assisted
684 Breeding. In: Bennetzen J, Flint-Garcia S, Hirsch C, Tuberosa R (eds) The Maize Genome. Springer
685 International Publishing, Cham, pp 367–388
- 686 Kadam DC, Potts SM, Bohn MO, et al (2016) Genomic Prediction of Single Crosses in the Early Stages of a Maize
687 Hybrid Breeding Pipeline. G3 Genes|Genomes|Genetics 6:3443–3453.
688 <https://doi.org/10.1534/g3.116.031286>
- 689 Kadam DC, Rodriguez OR, Lorenz AJ (2021) Optimization of training sets for genomic prediction of early-stage
690 single crosses in maize. Theor Appl Genet 134:687–699. <https://doi.org/10.1007/s00122-020-03722-w>

- 691 Laporte F, Charcosset A, Mary-Huard T (2022) Efficient ReML inference in variance component mixed models
692 using a Min-Max algorithm. *PLOS Computational Biology* 18:e1009659.
693 <https://doi.org/10.1371/journal.pcbi.1009659>
- 694 Laporte F, Mary-Huard T (2020) MM4LMM: Inference of Linear Mixed Models Through MM Algorithm
- 695 Legarra A, Gonzalez-Dieguez DO, Charcosset A, Vitezica ZG (2023) Impact of interpopulation distance on
696 dominance variance and average heterosis in hybrid populations within species. *Genetics* 224:iyad059.
697 <https://doi.org/10.1093/genetics/iyad059>
- 698 Lorenzi A, Bauland C, Mary-Huard T, et al (2022) Genomic prediction of hybrid performance: comparison of the
699 efficiency of factorial and tester designs used as training sets in a multiparental connected reciprocal
700 design for maize silage. *Theor Appl Genet.* <https://doi.org/10.1007/s00122-022-04176-y>
- 701 Maenhout S, De Baets B, Haesaert G (2010) Prediction of maize single-cross hybrid performance: support vector
702 machine regression versus best linear prediction. *Theoretical and applied genetics* 120:415–427
- 703 Mangin B, Rincent R, Rabier C-E, et al (2019) Training set optimization of genomic prediction by means of
704 EthAcc. *PLoS ONE* 14:e0205629. <https://doi.org/10.1371/journal.pone.0205629>
- 705 Merrick LF, Carter AH (2021) Comparison of genomic selection models for exploring predictive ability of
706 complex traits in breeding programs. *The Plant Genome* 14:e20158. <https://doi.org/10.1002/tpg2.20158>
- 707 Meuwissen THE, Hayes BJ, Goddard ME (2001) Prediction of Total Genetic Value Using Genome-Wide Dense
708 Marker Maps. *Genetics* 157:1819–1829
- 709 Michel S, Ametz C, Gungor H, et al (2016) Genomic selection across multiple breeding cycles in applied bread
710 wheat breeding. *Theor Appl Genet* 129:1179–1189. <https://doi.org/10.1007/s00122-016-2694-2>
- 711 Momen M, Morota G (2018) Quantifying genomic connectedness and prediction accuracy from additive and non-
712 additive gene actions. *Genetics Selection Evolution* 50:45. <https://doi.org/10.1186/s12711-018-0415-9>
- 713 Mrode RA, Thompson R (2005) Linear models for the prediction of animal breeding values, 2nd ed. CABI Pub,
714 Wallingford, UK ; Cambridge, MA
- 715 Neyhart JL, Tiede T, Lorenz AJ, Smith KP (2017) Evaluating Methods of Updating Training Data in Long-Term
716 Genomewide Selection. *G3 Genes|Genomes|Genetics* 7:1499–1510.
717 <https://doi.org/10.1534/g3.117.040550>
- 718 Pszczola M, Calus MPL (2016) Updating the reference population to achieve constant genomic prediction
719 reliability across generations. *animal* 10:1018–1024. <https://doi.org/10.1017/S1751731115002785>
- 720 Pszczola M, Strabel T, Mulder HA, Calus MPL (2012) Reliability of direct genomic values for animals with
721 different relationships within and to the reference population. *Journal of Dairy Science* 95:389–400.
722 <https://doi.org/10.3168/jds.2011-4338>
- 723 R Core Team (2020) R: A Language and Environment for Statistical Computing. R Foundation for Statistical
724 Computing, Vienna, Austria
- 725 Reif JC, Gumpert F-M, Fischer S, Melchinger AE (2007) Impact of Interpopulation Divergence on Additive and
726 Dominance Variance in Hybrid Populations. *Genetics* 176:1931.
727 <https://doi.org/10.1534/genetics.107.074146>
- 728 Revelle W (2021) psych: Procedures for Psychological, Psychometric, and Personality Research. Northwestern
729 University, Evanston, Illinois
- 730 Rincent R, Charcosset A, Moreau L (2017) Predicting genomic selection efficiency to optimize calibration set and
731 to assess prediction accuracy in highly structured populations. *Theor Appl Genet* 130:2231–2247.
732 <https://doi.org/10.1007/s00122-017-2956-7>

- 733 Rincent R, Laloë D, Nicolas S, et al (2012) Maximizing the Reliability of Genomic Selection by Optimizing the
734 Calibration Set of Reference Individuals: Comparison of Methods in Two Diverse Groups of Maize
735 Inbreds (*Zea mays* L.). *Genetics* 192:715–728. <https://doi.org/10.1534/genetics.112.141473>
- 736 Rio S, Akdemir D, Carvalho T, Sánchez JI y. (2022a) Assessment of genomic prediction reliability and
737 optimization of experimental designs in multi-environment trials. *Theor Appl Genet* 135:405–419.
738 <https://doi.org/10.1007/s00122-021-03972-2>
- 739 Rio S, Charcosset A, Mary-Huard T, et al (2022b) Building a Calibration Set for Genomic Prediction,
740 Characteristics to Be Considered, and Optimization Approaches. In: Ahmadi N, Bartholomé J (eds)
741 *Genomic Prediction of Complex Traits*. Springer US, New York, NY, pp 77–112
- 742 Sallam AH, Endelman JB, Jannink J-L, Smith KP (2015) Assessing Genomic Selection Prediction Accuracy in a
743 Dynamic Barley Breeding Population. *The Plant Genome* 8:plantgenome2014.05.0020.
744 <https://doi.org/10.3835/plantgenome2014.05.0020>
- 745 Schrag TA, Melchinger AE, Sørensen AP, Frisch M (2006) Prediction of single-cross hybrid performance for grain
746 yield and grain dry matter content in maize using AFLP markers associated with QTL. *Theoretical and*
747 *Applied Genetics* 113:1037–1047. <https://doi.org/10.1007/s00122-006-0363-6>
- 748 Schrag TA, Westhues M, Schipprack W, et al (2018) Beyond genomic prediction: combining different types of
749 omics data can improve prediction of hybrid performance in maize. *Genetics* 208:1373–1385
- 750 Seye AI (2019) Prédiction assistée par marqueurs de la performance hybride dans un schéma de sélection
751 réciproque : simulations et évaluation expérimentale pour le maïs ensilage. Thesis, Paris Saclay
- 752 Seye AI, Bauland C, Charcosset A, Moreau L (2020) Revisiting hybrid breeding designs using genomic
753 predictions: simulations highlight the superiority of incomplete factorials between segregating families
754 over topcross designs. *Theor Appl Genet* 133:1995–2010. <https://doi.org/10.1007/s00122-020-03573-5>
- 755 Seye AI, Bauland C, Giraud H, et al (2019) Quantitative trait loci mapping in hybrids between Dent and Flint
756 maize multiparental populations reveals group-specific QTL for silage quality traits with variable
757 pleiotropic effects on yield. *Theor Appl Genet* 132:1523–1542. <https://doi.org/10.1007/s00122-019-03296-2>
- 759 Stuber CW, Cockerham CC (1966) GENE EFFECTS AND VARIANCES IN HYBRID POPULATIONS.
760 *Genetics* 54:1279–1286. <https://doi.org/10.1093/genetics/54.6.1279>
- 761 Surault F, Emile JC, Briand M, et al (2005) Variabilité génétique de la digestibilité in vivo d'hybrides de maïs.
762 Bilan de 34 années de mesures. *Fourrages* 183:459
- 763 Technow F, Bürger A, Melchinger AE (2013) Genomic Prediction of Northern Corn Leaf Blight Resistance in
764 Maize with Combined or Separated Training Sets for Heterotic Groups. *G3* 3:197–203.
765 <https://doi.org/10.1534/g3.112.004630>
- 766 Technow F, Schrag TA, Schipprack W, et al (2014) Genome Properties and Prospects of Genomic Prediction of
767 Hybrid Performance in a Breeding Program of Maize. *Genetics* 197:1343–1355.
768 <https://doi.org/10.1534/genetics.114.165860>
- 769 VanRaden PM (2008) Efficient Methods to Compute Genomic Predictions. *Journal of Dairy Science* 91:4414–
770 4423. <https://doi.org/10.3168/jds.2007-0980>
- 771 Varona L, Legarra A, Toro MA, Vitezica ZG (2018) Non-additive Effects in Genomic Selection. *Front Genet* 9:78.
772 <https://doi.org/10.3389/fgene.2018.00078>
- 773 Vitezica ZG, Legarra A, Toro MA, Varona L (2017) Orthogonal Estimates of Variances for Additive, Dominance,
774 and Epistatic Effects in Populations. *Genetics* 206:1297–1307.
775 <https://doi.org/10.1534/genetics.116.199406>

- 776 Vitezica ZG, Varona L, Legarra A (2013) On the Additive and Dominant Variance and Covariance of Individuals
 777 Within the Genomic Selection Scope. *Genetics* 195:1223–1230.
 778 <https://doi.org/10.1534/genetics.113.155176>
- 779 Wang N, Wang H, Zhang A, et al (2020) Genomic prediction across years in a maize doubled haploid breeding
 780 program to accelerate early-stage testcross testing. *Theor Appl Genet* 133:2869–2879.
 781 <https://doi.org/10.1007/s00122-020-03638-5>
- 782 Williams E, Piepho H-P, Whitaker D (2011) Augmented p-rep designs. *Biom J* 53:19–27.
 783 <https://doi.org/10.1002/bimj.201000102>
- 784 Williams EJ (1959) 136. Query: Significance of Difference between Two Non-Independent Correlation
 785 Coefficients. *Biometrics* 15:135. <https://doi.org/10.2307/2527608>
- 786 Zhao Y, Gowda M, Liu W, et al (2012) Accuracy of genomic selection in European maize elite breeding
 787 populations. *Theor Appl Genet* 124:769–776. <https://doi.org/10.1007/s00122-011-1745-y>
- 788 Zhong S, Dekkers JCM, Fernando RL, Jannink J-L (2009) Factors Affecting Accuracy From Genomic Selection
 789 in Populations Derived From Multiple Inbred Lines: A Barley Case Study. *Genetics* 182:355–364.
 790 <https://doi.org/10.1534/genetics.108.098277>

791 **Statements and declarations**

792 **Funding**

793 Lidea, Limagrain Europe, Maïsadour Semences, Corteva, RAGT 2n, KWS and Syngenta Seeds grouped in the
 794 frame of the ProMais association funded the SAM-MCR project. A.L. PhD contract was funded by RAGT 2n and
 795 ANRT contract n°660 2020/0032, with contributions of all SAM-MCR project partners. GQE-Le Moulon benefits
 796 from the support of Saclay Plant Sciences-SPS (ANR-17-EUR-0007).

797 **Competing Interests**

798 The authors have no relevant financial or non-financial interests to disclose.

799 **Author's contributions**

800 CB, AC and LM initiated this project. LM and CB coordinated it with the help of GT and CG. AC and LM
 801 supervised this work with contributions of TMH. SP, and CP contributed to the multiplication of DH lines and
 802 hybrid seeds production. DM and VC prepared DNA samples for the genotyping of the inbred lines and assembled
 803 the genotypic data. AL analyzed the results and prepared the manuscript. All authors discussed the results and
 804 contributed to the final manuscript. All authors revised and approved the manuscript.

805 **Data availability**

806 The datasets generated during and/or analyzed during the current study are available from the corresponding author
807 on reasonable request.

808 **Ethics approval**

809 All usual standards have been respected.

810 **Consent to participate**

811 Not relevant for this study on plants.

812 **Consent to publish**

813 Not relevant for this study on plants.

814

815 **Figure legends**

816 **Fig. 1** Hybrid experimental designs produced by crossing inbred lines from the initial generation (G0) and the
817 inbred lines obtained after one cycle of selection (G1).

818 **Fig. 2** Predictive abilities obtained by cross-validations within the 442 G1 hybrids using different prediction
819 models (PBLUP, GCA.1, GCA.2 or G models) in Scenario 1. The mean predictive ability over the 100 replicates
820 is represented by a white cross. Significant differences (as obtained by paired t-tests at a level risk $\alpha=0.05$) are
821 indicated with letters: two different letters indicate a significant difference and at least one common letters indicate
822 no significant difference.

823 **Fig. 3** Predictive abilities obtained in Scenario 2a when training the GS model on the G0_F-1H design (951
824 hybrids) to predict the 47 G0S hybrids or the 442 G1 hybrids. The dotted line corresponds to the mean predictive
825 ability over 100 replicates of cross-validations within the 442 G1 hybrids.

826 **Fig. 4** Predictive abilities obtained for the G1 hybrids (442) by training the GS model on the G0_F-4H (363) or
827 the G0_T (360) TRSs in Scenario 2b. Williams tests were performed ($\alpha=0.05$) and significant differences were
828 indicated with letters: two different letters indicate a significant difference and at least one common letters indicate
829 no significant difference.

830 **Fig. 5** Predictive abilities obtained in Scenario 2b' by training the GS model on 180 hybrids issued from tester-
831 based or factorial TRSs to predict the G1 hybrids (442). The different tester-based TRSs correspond to: 90 lines
832 crossed to one tester (1T-180H-180L-A, 1T-180H-180L-B, 1T-180H-180L-C, 1T-180H-180L-D), 90 lines
833 crossed to two testers (2T-180H-180L), 45 lines crossed to two testers (2T-180H-90L). The factorial design (F-
834 180H-152L) corresponds to the crosses of 76 flint lines with 76 dent lines. The sampling was repeated 10 times
835 and t-tests ($\alpha=0.05$) were performed for the F-180H-170L, 2T-180H-180L and 2T-180H-90L. Significant
836 differences were indicated with letters: two different letters indicate a significant difference and at least one
837 common letters indicate no significant difference.

838 **Fig. 6** Predictive abilities obtained in Scenario 3a when predicting one-fifth of the G1 hybrids (88) using different
839 TRSs: G0R hybrids (in solid colored lines) completed by 132 G0S hybrids (in dotted colored lines) and m G1
840 hybrids (with m ranging from 0 to 354 from the left to the right of each graph). The mean predictive ability over
841 100 replicates is represented by a dot for each TRS. The number of hybrids in the initial G0R TRSs is indicated
842 between brackets in the figure legend.

843 **Fig. 7** Predictive abilities obtained with TRSs composed of an initial G0 set (1360 hybrids) completed by a
844 CDmean optimized G1 hybrid set of different sizes (50, 100, 200 and 300). The G1 hybrid set is optimized
845 considering only G1 information (CDmean 1) or considering G1 and G0 information (CDmean 2) in the calculation
846 of the CDmean and compared to a randomly sampled TRS (Random). The white cross represents the mean
847 predictive ability over the 100 replicates.

848

849 **Table 1** Description of all experimental designs used in this study.

Years of phenotyping	Breeding cycle	Design	Name	Hybrids within the design ^a	Reference ^c
2013, 2014	G0	Factorial	G0_F-1H	G0R ^a	Giraud et al. 2017a, b; Seye et al. 2019; Lorenzi et al. 2022
2016, 2017	G0	Factorial	G0_F-4H	G0R + G0S ^b	Seye 2019; Lorenzi et al. 2022
		Tester	G0_T		
2019, 2020	G0+G1	Factorial	(G0S+G1)_F-1H	G0S + G1	Current study

850 ^a G0R hybrids were produced by crossing two random lines from the G0 cycle

851 ^b G0S hybrids were produced by crossing two selected lines from the G0 cycle

852 ^c A reference was indicated for data that was already analyzed in previous studies

853

854 **Table 2** Definition of the genomic prediction models tested in Scenario 1.

Models	Model code	Random genetic effects ^a	Reference
PBLUP		g	Henderson 1976
GCA.1	GCA	$g_{GCA_f} + g_{GCA_d}$	VanRaden 2008
	GCA_SCA	$g_{GCA_f} + g_{GCA_d} + g_{SCA}$	
GCA.2	GCA:A	$g_{A_f} + g_{A_d} + r$	González-Diéguéz et al. 2021
	GCA:AD	$g_{A_f} + g_{A_d} + g_D$	
	GCA:A(AAdf)	$g_{A_f} + g_{A_d} + g_{AA_{df}}$	
	GCA:AD(AAdf)	$g_{A_f} + g_{A_d} + g_D + g_{AA_{df}}$	
	GCA:AD(AAf)(AAd)(AAdf)	$g_{A_f} + g_{A_d} + g_D + g_{AA_f} + g_{AA_d} + g_{AA_{df}}$	
G	G:A	g_A	Vitezica et al. 2017
	G:AD	$g_A + g_D$	
	G:A(AA)	$g_A + g_{AA}$	
	G:AD(AA)	$g_A + g_D + g_{AA}$	

855 ^a The list of the random genetic effects considered in the GCA models correspond to: dent GCA (g_{GCA_d}), flint
856 GCA (g_{GCA_f}), SCA (g_{SCA}), intragroup additive-by-additive epistasis for the dent (g_{AA_d}) and flint group (g_{AA_f}),
857 and intergroup additive-by-additive epistasis ($g_{AA_{df}}$) effects. In the G models, random genetic effects correspond
858 to: additive (g_A), dominance (g_D) and additive-by-additive epistasis (g_{AA}) effects.

859

860 **Table 3** Broad-sense heritability (H^2), percentage of genetic variance assigned to SCA variance (%SCA) and
 861 variance components estimated on phenotypic data corrected for spatial effects for the (G0S+G1)_F-1H without
 862 marker information.

	DMY (t/ha)		DMC (%)		DtSilk (days)		MFU (MFUx10 ² /kg)	
	G0S	G1	G0S	G1	G0S	G1	G0S	G1
$\sigma_{GCA_f}^2$	0.50(0.24) ^d	0.31(0.05)	0.46(0.28)	1.47(0.21)	1.63(0.71)	2.06(0.29)	0.44(0.24)	0.49(0.09)
$\sigma_{GCA_d}^2$	0.13(0.18)	0.25(0.05)	1.42(0.51)	0.73(0.21)	1.57(0.65)	1.41(0.27)	0.00	0.36(0.09)
σ_{SCA}^2	0.14(0.18)	0.00	0.00	0.25(0.20)	0.03(0.27)	0.05(0.22)	0.19(0.13)	0.00(0.09)
$\sigma_{GCA_f \times E}^2$	0.07(0.08)	0.05(0.05)	0.00	0.11(0.05)	0.41(0.16)	0.17(0.07)	0.27(0.17)	0.20(0.07)
$\sigma_{GCA_d \times E}^2$	0.12(0.09)	0.07(0.04)	0.39(0.13)	0.31(0.05)	0.05(0.12)	0.09(0.06)	0.06(0.12)	0.13(0.07)
$\sigma_{SCA \times E}^2$	0.00	0.23(0.07)	0.00	0.00	0.00	0.24(0.11)	0.00	0.11(0.09)
σ_E^2 ^a	0.31(0.05)-1.40(0.12)		0.57(0.07)-3.62(0.27)		0.64(0.09)-2.33(0.20)		0.12(0.02)-7.97(0.55)	
%SCA ^b	19	0	0	10	1	1	30	0
H^2 ^c	0.87	0.80	0.90	0.92	0.93	0.94	0.56	0.62

863 ^a Minimum and maximum residual variance across all environments

864 ^b Percentage of SCA variance computed as $\frac{\sigma_{SCA}^2}{\sigma_{GCA_d}^2 + \sigma_{GCA_f}^2 + \sigma_{SCA}^2} \times 100$

865 ^c Broad-sense heritability

866 ^d Standard error in brackets

867

868 **Table 4** Performances (ls-means) of commercial, founder and experimental hybrids (G0S and G1 hybrids) and
 869 genetic gain of the experimental hybrids compared to the founder hybrids corresponding to the (G0S+G1)_F-1H
 870 design.

	Hybrid type	Component	DMY (t/ha)	DMC (%)	DtSilk (days)	MFU (MFUx10 ² /kg)
LS-means	Commercial	Mean	17.96 (17.18-18.74) ^b	34.69 (34.37-35.00)	201.89 (200.27-203.50)	95.54 (95.34-95.74)
		Sd^c	1.10	0.45	2.28	0.28
	Founder	Mean	15.80 (14.27-17.47)	34.10 (30.53-37.48)	203.14 (199.80-206.16)	95.28 (91.13-98.14)
		Sd	0.84	1.94	1.50	2.05
	G0S	Mean	17.35 (14.82-18.89)	33.33 (30.54-37.13)	204.97 (201.80-208.79)	93.17 (89.04-97.06)
		Sd	0.92	1.40	1.82	1.56
	G1	Mean	17.33 (14.33-19.72)	33.43 (29.39-39.18)	205.04 (197.98-211.40)	93.13 (87.59-101.36)
		Sd	0.85	1.63	1.97	1.71
Genetic gain^a	G0S		1.55	-0.77	1.83	-2.11
	G1		1.52	-0.67	1.90	-2.15
Predicted genetic gain^d	G0S		1.45	-0.33	1.18	-1.35
	G1		1.41	-0.28	0.91	-1.14

871 ^a Genetic gain computed as the difference between the mean performance of the experimental hybrids and the
 872 founder hybrids

873 ^b Minimum and maximum mean performance in brackets

874 ^c Standard deviation of the ls-means of the experimental hybrid performances

875 ^d Predicted genetic gain based on genomic predictions trained on the G0_F-1H

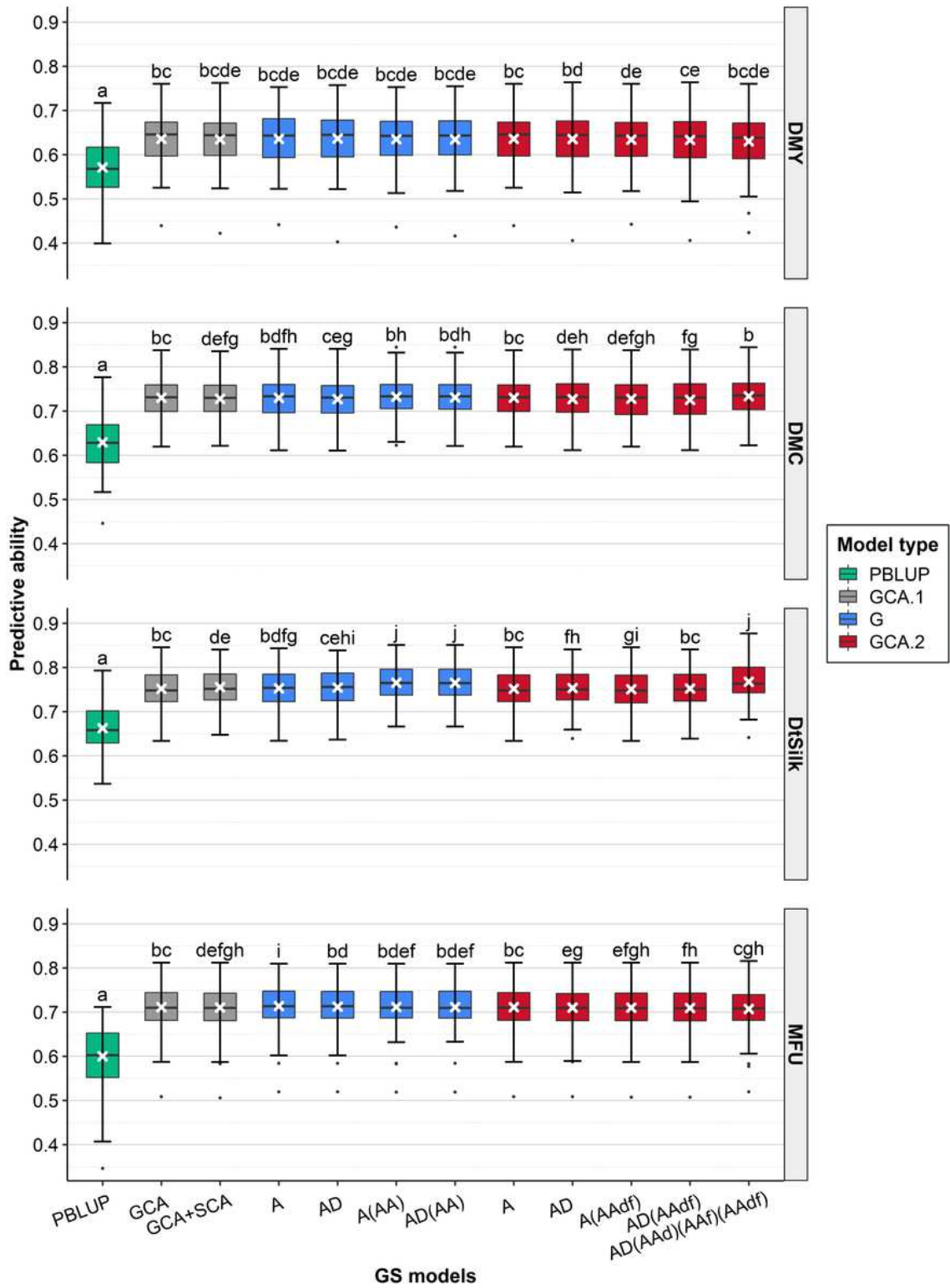


Figure 2

Predictive abilities obtained by cross-validations within the 442 G1 hybrids using different prediction models (PBLUP, GCA.1, GCA.2 or G models) in Scenario 1. The mean predictive ability over the 100 replicates is represented by a white cross. Significant differences (as obtained by paired t-tests at a level risk $\alpha=0.05$) are indicated with letters: two different letters indicate a significant difference and at least one common letters indicate no significant difference.

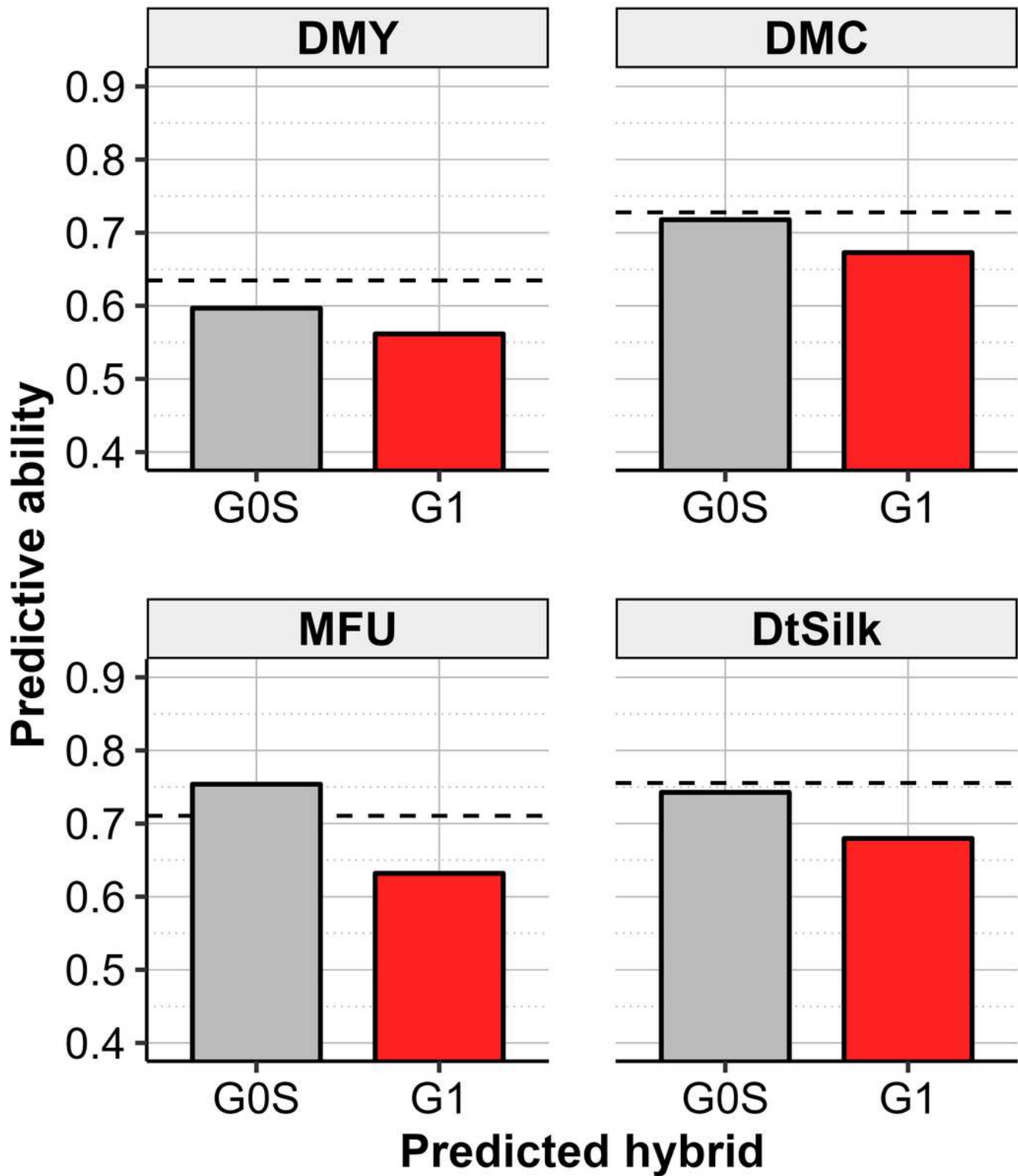


Figure 3

Predictive abilities obtained in Scenario 2a when training the GS model on the G0_F-1H design (951 hybrids) to predict the 47 G0S hybrids or the 442 G1 hybrids. The dotted line corresponds to the mean predictive ability over 100 replicates of cross-validations within the 442 G1 hybrids.

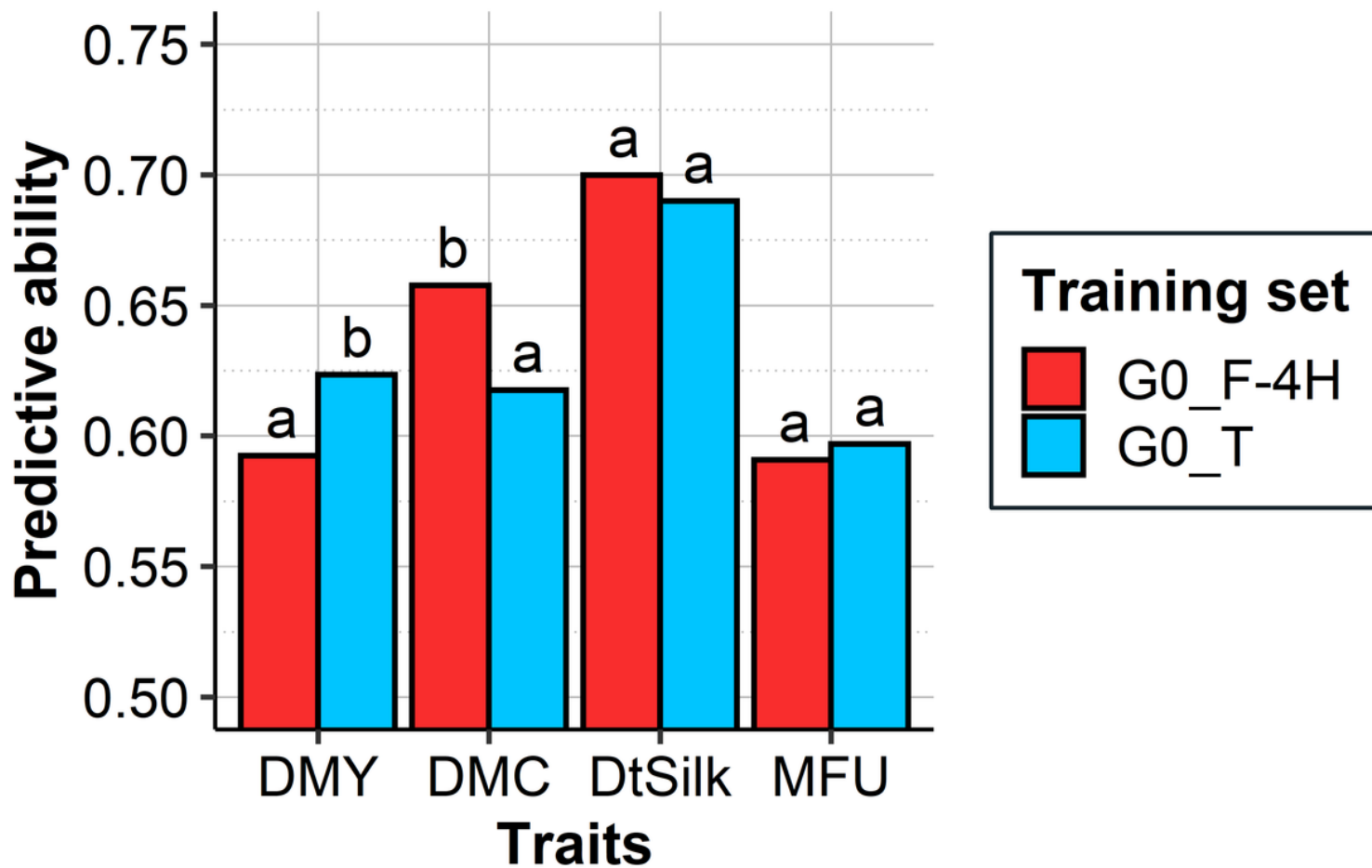


Figure 4

Predictive abilities obtained for the G1 hybrids (442) by training the GS model on the G0_F-4H (363) or the G0_T (360) TRSs in Scenario 2b. Williams tests were performed ($\alpha=0.05$) and significant differences were indicated with letters: two different letters indicate a significant difference and at least one common letters indicate no significant difference.

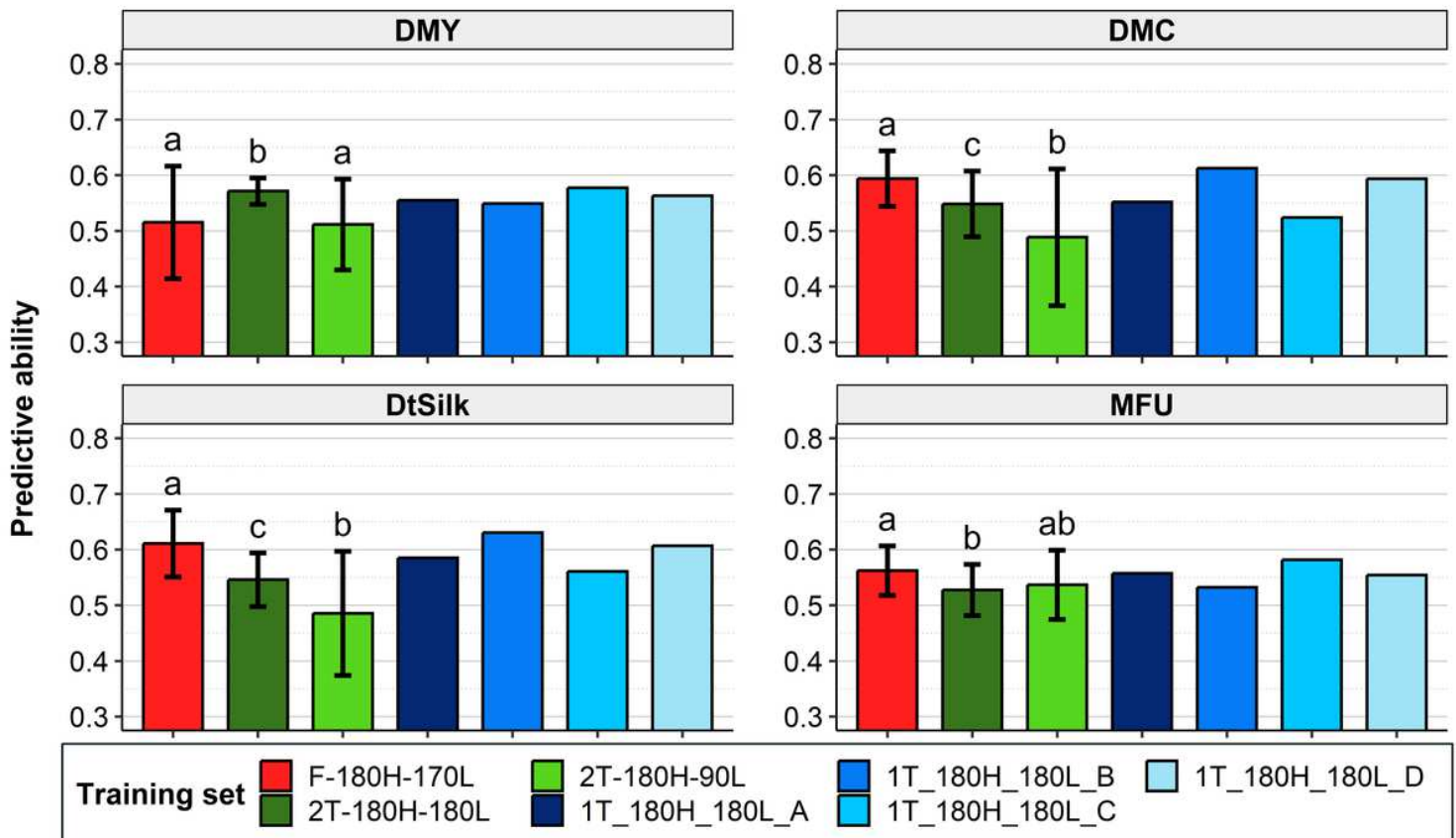


Figure 5

Predictive abilities obtained in Scenario 2b' by training the GS model on 180 hybrids issued from tester-based or factorial TRSs to predict the G1 hybrids (442). The different tester-based TRSs correspond to: 90 lines crossed to one tester (1T-180H-180L-A, 1T-180H-180L-B, 1T-180H-180L-C, 1T-180H-180L-D), 90 lines crossed to two testers (2T-180H-180L), 45 lines crossed to two testers (2T-180H-90L). The factorial design (F-180H-152L) corresponds to the crosses of 76 flint lines with 76 dent lines. The sampling was repeated 10 times and t-tests ($\alpha=0.05$) were performed for the F-180H-170L, 2T-180H-180L and 2T-180H-90L. Significant differences were indicated with letters: two different letters indicate a significant difference and at least one common letters indicate no significant difference.

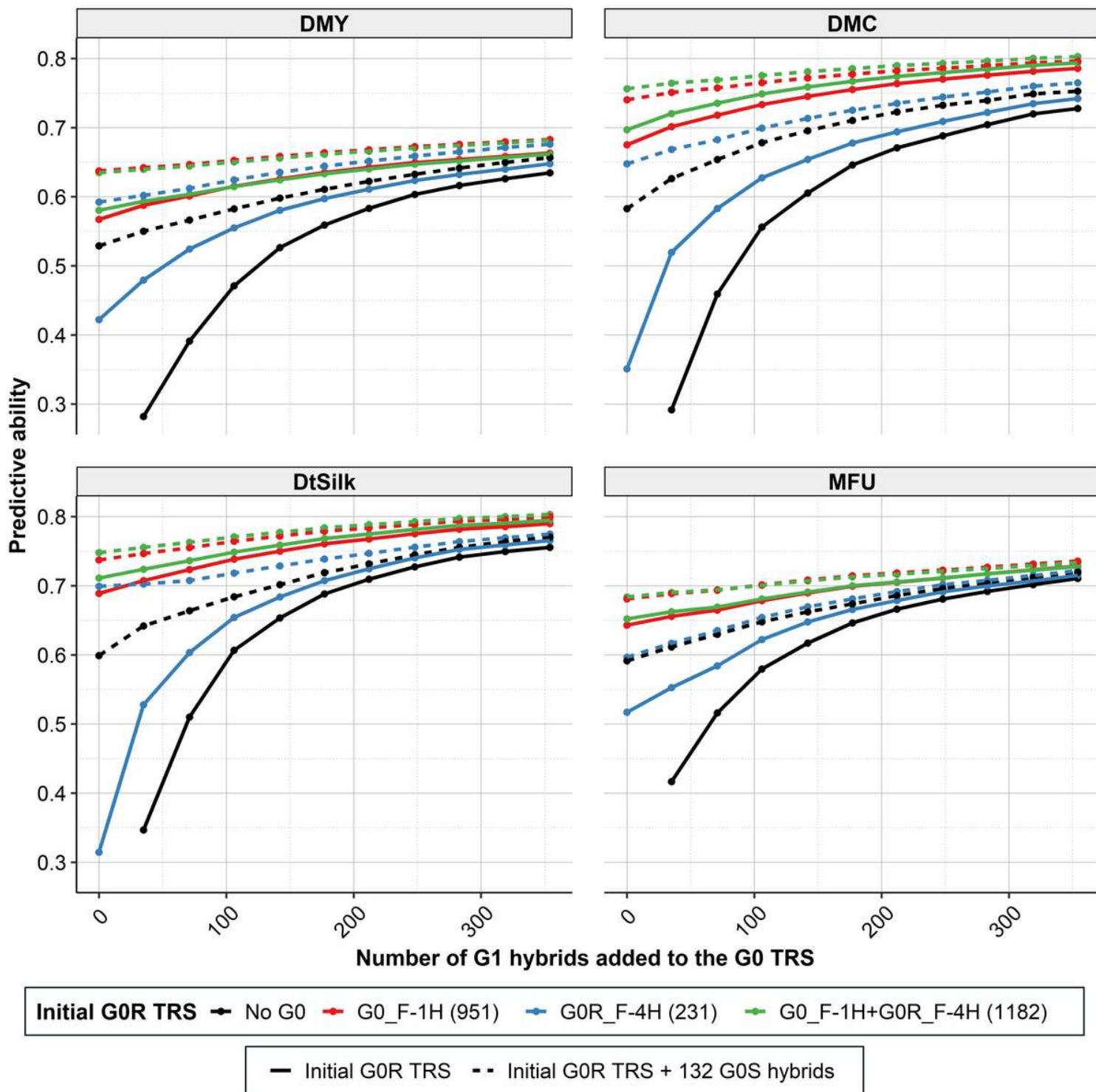


Figure 6

Predictive abilities obtained in Scenario 3a when predicting one-fifth of the G1 hybrids (88) using different TRSs: G0R hybrids (in solid colored lines) completed by 132 G0S hybrids (in dotted colored lines) and m G1 hybrids (with m ranging from 0 to 354 from the left to the right of each graph). The mean predictive ability over 100 replicates is represented by a dot for each TRS. The number of hybrids in the initial G0R TRSs is indicated between brackets in the figure legend.

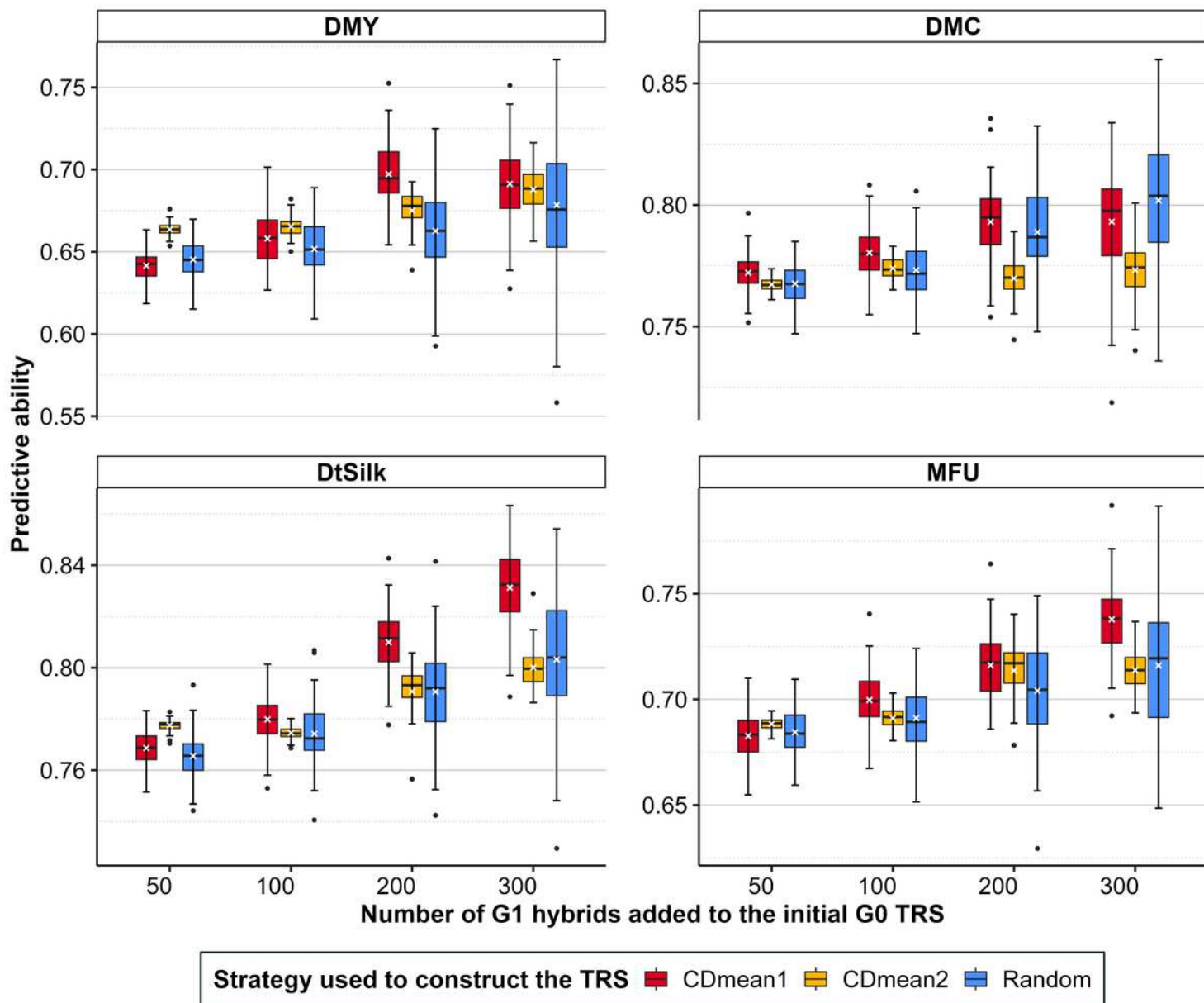


Figure 7

Predictive abilities obtained with TRSs composed of an initial G0 set (1360 hybrids) completed by a CDmean optimized G1 hybrid set of different sizes (50, 100, 200 and 300). The G1 hybrid set is optimized considering only G1 information (CDmean 1) or considering G1 and G0 information (CDmean 2) in the calculation of the CDmean and compared to a randomly sampled TRS (Random). The white cross represents the mean predictive ability over the 100 replicates.

Supplementary Files

This is a list of supplementary files associated with this preprint. Click to download.

- [20230529SupplementaryMaterial.pdf](#)